A review of deformation bands in reservoir sandstones: geometries, mechanisms and distribution

HAAKON FOSSEN[1,2,3]*, ROGER SOLIVA[4], GREGORY BALLAS[5], BARBARA TRZASKOS[2], CAROLINA CAVALCANTE[2] & RICHARD A. SCHULTZ[6]

[1]*Department of Earth Science and Museum of Natural History, University of Bergen, Postboks 7803, 5007 Bergen, Norway*

[2]*Departamento de Geologia, Universidade Federal do Paraná – Setor de Ciências da Terra, Caixa Postal 19.001, Centro Politécnico - Jardim das Américas, 81531-980 Curitiba, PR, Brazil*

[3]*Instituto de Geociências, Universidade de São Paulo, 05508-900, SP, Brazil*

[4]*Geosciences Montpellier, Université de Montpellier, Campus Triolet, CC060, Place Eugène, Bataillon, 34095 Montpellier Cedex 05, France*

[5]*Institut Français de Recherche pour l'Exploitation de la Mer, Pointe du Diable, 29280 Plouzané, France*

[6]*Petroleum and Geosystems Engineering, The University of Texas at Austin, Austin Texas 78712 USA*

**Correspondence: haakon.fossen@uib.no*

Abstract: Deformation bands are common subseismic structures in porous sandstones that vary with respect to deformation mechanisms, geometries and distribution. The amount of cataclasis involved largely determines how they impact fluid flow, and cataclasis is generally promoted by coarse grain size, good sorting, high porosity and overburden (usually >500–1000 m). Most bands involve a combination of shear and compaction, and a distinction can be made between those where shear displacement greatly exceeds compaction (compactional shear bands or CSB), where the two are of similar magnitude (shear-enhanced compaction bands or SECB), and pure compaction bands (PCB). The latter two only occur in the contractional regime, are characterized by high (70–100°) dihedral angles (SECB) or perpendicularity (PCB) to σ_1 (the maximum principal stress) and are restricted to layers with very high porosity. Contraction generally tends to produce populations of well-distributed deformation bands, whereas in the extensional regime the majority of bands are clustered around faults. Deformation bands also favour highly porous parts of a reservoir, which may result in a homogenization of the overall reservoir permeability and enhance sweep during hydrocarbon production. A number of intrinsic and external variables must therefore be considered when assessing the influence of deformation bands on reservoir performance.

The mechanisms by which highly porous sediments and rocks such as sand and sandstone respond to deformation differ fundamentally from that of low-porosity and non-porous rocks. In particular, these sediments and rocks form subseismic strain-localization features known as deformation bands (Aydin 1978; Davis 1999; Fossen *et al.* 2007) instead of fractures. Deformation bands (Fig. 1a) differ from classical fractures in several ways, notably: (1) their generally compactive nature that leads to porosity loss and permeability reduction; and (2) the limited ability of individual bands to accumulate displacement, resulting in formation of large populations of bands or band clusters. These and several other characteristic properties of deformation bands relate to the high porosity of the host rock, which allows for reorganization of grains and grain fragments during deformation. Furthermore, the observation that most deformation bands reduce porosity and permeability makes it interesting to consider their impact on fluid flow during hydrocarbon production.

In this work we present a review of deformation bands, their characteristic geometric and petrophysical properties, and the ways that they occur in different tectonic settings. The many factors influencing the occurrence and type of deformation bands make prediction of such structures difficult

From: Ashton, M., Dee, S. J. & Wennberg, O. P. (eds) *Subseismic-Scale Reservoir Deformation*. Geological Society, London, Special Publications, **459**, https://doi.org/10.1144/SP459.4

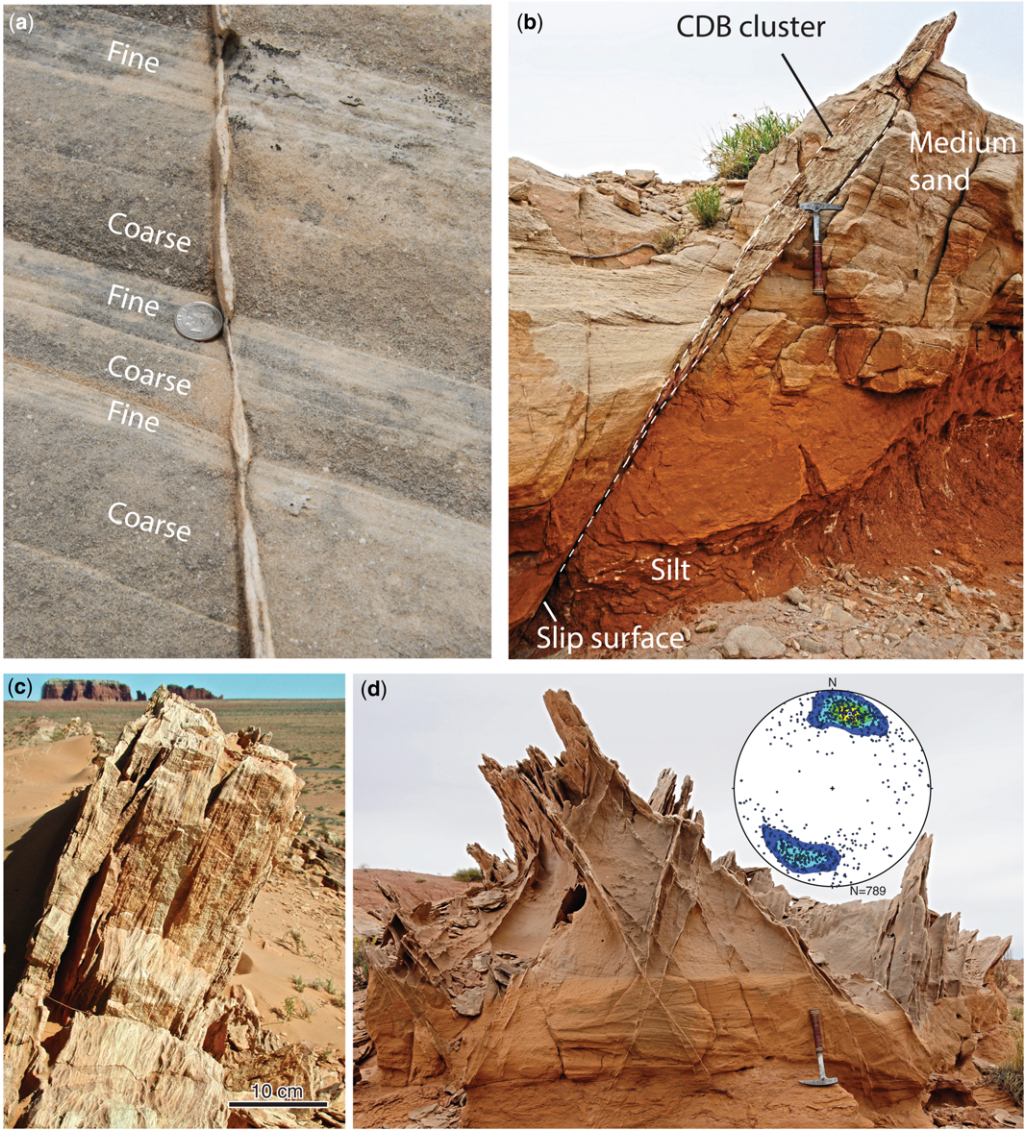

Fig. 1. Examples of deformation bands in the extensional regime. (**a**) Compactional shear band (CSB) showing thickness variation between fine to coarse layers. Navajo Sandstone, Waterpocket monocline, Utah. (**b**) Cluster of CSB transitioning into a slip surface in the fine-grained sand/siltstone in the lower part of the picture. (**c**) Thick deformation band cluster (CSB). (**d**) Conjugate CSB in Entrada Sandstone, with lower-hemisphere equal-area projection of poles to deformation bands in the Mollys Castle–Goblin Valley area, south Utah. Two maxima suggest an average dihedral angle of 47°. (b–d) from Entrada Sandstone in the Goblin Valley area, San Rafael Desert, Utah.

in detail, but some general statements and 'rules' can be made. The purpose of this work is to explore and review the most important of those factors and to try to extract general conclusions that can help us understand when, where and how deformation bands form, how they are distributed and their properties with respect to fluid flow (Ballas *et al.* 2015). Based on this general knowledge, it should be possible to make at least some first-order predictions about the occurrence and nature of these subseismic-scale strain-localization features in subsurface reservoirs, even where well data are scarce.

Band types, deformation mechanisms and kinematics

Deformation bands are strain-localization structures that develop in porous media, notably sandstones and conglomerates. They form in the full range of tectonic regimes, from pure extension to strike-slip to contraction, provided that the sediment or rock had sufficiently high porosity at the time of deformation, generally more than *c.* 15%. While the term deformation band has been used in a general way to denote strain-localization structures formed in a variety of rock types (e.g. Cobbold 1977) and in a more specific way to describe intracrystalline bands of dislocation structures in plastically deformed rocks (Passchier & Trouw 2005), the use of the term for millimetre- to centimetre-wide tabular deformation structures in highly porous rocks was introduced primarily by Aydin (1978) and Aydin & Johnson (1978, 1983). This is now well entrenched in the geological literature and textbooks (Davis *et al.* 2012; Fossen 2016).

Kinematic classes and their relation to deformation mechanism

As has previously been pointed out (Fossen *et al.* 2007), deformation bands can be classified according to kinematics or deformation mechanism. Deformation mechanisms are extremely important, both mechanically and with regard to porosity and permeability changes. The most important factor is the amount of cataclasis involved. Cataclasis typically generates a mechanically strong and stiff internal (ultra)cataclastic rock that involves compaction and reduction in porosity and permeability by up to several orders of magnitude together with some dissolution and cementation (see review by Ballas *et al.* 2015). Cataclasis is to some extent related to kinematics and strain and, given that our understanding of the kinematic aspects of deformation bands has evolved over the last few years, we focus here on deformation band kinematics and the role of cataclasis.

The deformation bands described by Aydin in his initial papers from the San Rafael Desert in Utah are shear dominated, but involve a significant amount of grain crushing and thereby a component of band-perpendicular compaction. As deformation bands have been increasingly recognized in practically all parts of the world and in many tectonic settings, it has become clear that most deformation bands develop in the kinematic spectrum between simple shear (constant-volume or isochoric shear bands) and pure compaction (pure compaction bands), although most commonly with a predominant shear component (shear bands; Fig. 2). Furthermore, the impression has recently emerged that deformation bands tend to organize themselves into kinematic subsets along the shear-compaction spectrum, as discussed below. Deformation band formation also involves different microscale deformation mechanisms, namely cataclasis or grain

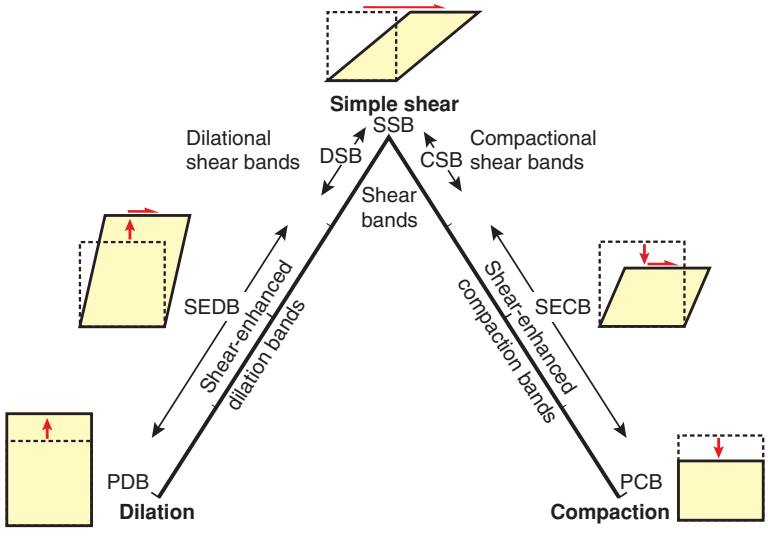

Fig. 2. Kinematic spectrum of deformation bands between the end-members compaction, simple shear and dilation. PCB: pure compaction band; SECB: shear-enhanced compaction band; CSB: compactional shear band; SSB: simple shear band (or simply shear band); DSB: dilational shear band; SEDB: shear-enhanced dilation band; PDB: pure dilation band.

crushing, frictional grain sliding and rotation, pressure solution (dissolution) and cementation. Of these, cataclasis, rotation and frictional sliding occur synkinematically, whereas cementation and pressure solution are relatively slow processes that can occur both during, after and sometimes long after band formation (Ngwenya *et al.* 2000; Philit *et al.* 2015).

The most common kinds of deformation bands are those dominated by shear (band-parallel) displacement with or without some additional compaction or dilation, and are collectively referred to as shear bands (Aydin *et al.* 2006). Bands that deform by simple shear (isochoric or simple shear bands) are limited to non-cataclastic bands where grains roll and slide (i.e. deform by rigid rotation and translation). In detail, intermittent episodes of minute dilation and compaction are necessary for well-packed grains to move past each other; dilation and compaction generally cancel each other out over time however, and are therefore of minor importance. Simple shear bands show no notable change in porosity as compared to the host rock unless phyllosilicate minerals are realigned along the band (e.g. Fossen 2010), although the formation of force chains that initiate oblique to the band walls may change the structure of the grain framework (Eichhubl *et al.* 2010; Cilona *et al.* 2012; Ballas *et al.* 2013; Soliva *et al.* 2013; Rodrigues *et al.* 2015).

Cataclastic shear bands always involve some compaction and therefore deviate from simple shear to form compactional shear bands (CSB, also called compactive shear bands) (Aydin *et al.* 2006; Fossen *et al.* 2007; Soliva *et al.* 2013). In these bands the shear displacement can be considerably larger than the compaction displacement. For instance, the classical cataclastic deformation bands described by Aydin (1978) typically show individual shear displacements up to a few centimetres (Fossen & Hesthammer 1997) and thicknesses of *c.* 1 mm. These kinds of cataclastic deformation bands typically involve a change in porosity from 25% in pristine sandstone to 10–15% in the deformation bands (Aydin & Johnson 1978; Torabi & Fossen 2009), which implies approximately 0.13–0.2 mm (13–20%) compaction for a 1 mm thick band. The shear displacement is therefore typically some two orders of magnitude higher than the compaction displacement for this type of shear band.

The amount of compaction across a compactional shear band increases with both its thickness and the amount of cataclasis involved. Interestingly, individual CSB of the type found in Triassic–Jurassic sandstones on the Colorado Plateau, Utah do not show any significant increase in thickness with increasing shear displacement (Fig. 3). The same is observed for CSB from the Nubian Sandstone in Sinai, Egypt (Rotevatn *et al.* 2008), that is, shear displacement is accumulated through continued cataclasis and grain reorganization, until a displacement of a few centimetres is achieved. Shearing can result in shear strains (γ) as high as $\gamma = 35$ for individual CSB in Utah, and considerably higher for bands in the Nubian Sandstone in Sinai that reach higher shear offsets and stronger cataclasis. At such high shear strains the maximum finite shortening (along the *Z*-axis of the strain ellipse) is very high (e.g. $1 + e_3 = 0.1$ for a 1 mm thick band with 10 mm offset (the band-perpendicular strain e_3)), which generates significant grain crushing. Note that this shortening is oblique to the band and therefore different from the band-perpendicular component discussed above. An important consequence is that CSB with high S/C (shear/compaction) ratios (see Fig. 4) show more intense comminution, producing ultra-cataclasis, than bands with a strong band-perpendicular compactional component (low S/C ratio, producing crush micro-breccias) (Ballas *et al.* 2012; Soliva *et al.* 2013).

It has been shown that classical Utah CSB define a square root dependence of maximum shear displacement (D_{max}) and length (L) of the form $D_{max} = \alpha L^{0.5}$, where α is a constant, so that they become very long relative to their small shear displacements (Fossen & Hesthammer 1997; Schultz *et al.* 2008). Once the CSB reaches a certain shear offset (a few centimetres), it can in some cases develop an internal striated slip surface, which is a very thin (*c.* 0.1 mm) zone of microcataclasite within the band that can then accumulate much larger (decimetre- or metre-scale) shear offsets. Examples of such bands have been observed in the Goblin Valley area, Utah (Entrada Sandstone), San Rafael Reef (Navajo Sandstone; Zuluaga *et al.* 2014) and Sinai (Nubian Sandstone; Rotevatn *et al.* 2008). With this type of development the kinematics become close to simple shear because porosity is now very small (*c.*1%) in the ultracataclastic zone that represents the slip surface, with almost no room for further compaction. It is not clear exactly what favours the formation of slip surfaces in single CSB, but they are found in well-sorted quartz sandstones deformed at $\geq$1.5 km depth in both the extensional and contractional regimes.

The most common development, however, is for the single CSB to become inactive as a new band forms alongside the first. This process, which most authors attribute to strain hardening (Rudnicki & Rice 1975; Aydin & Johnson 1978, 1983; Underhill & Woodcock 1987; Antonellini *et al.* 1994; Antonellini & Pollard 1995; Schultz & Balasko 2003; Shipton & Cowie 2003) although other models have been suggested (Nicol *et al.* 2013), repeats itself and leads to zones or clusters of deformation bands that can reach several decimetres in thickness in highly porous sandstones (Fig. 1b, c). During this

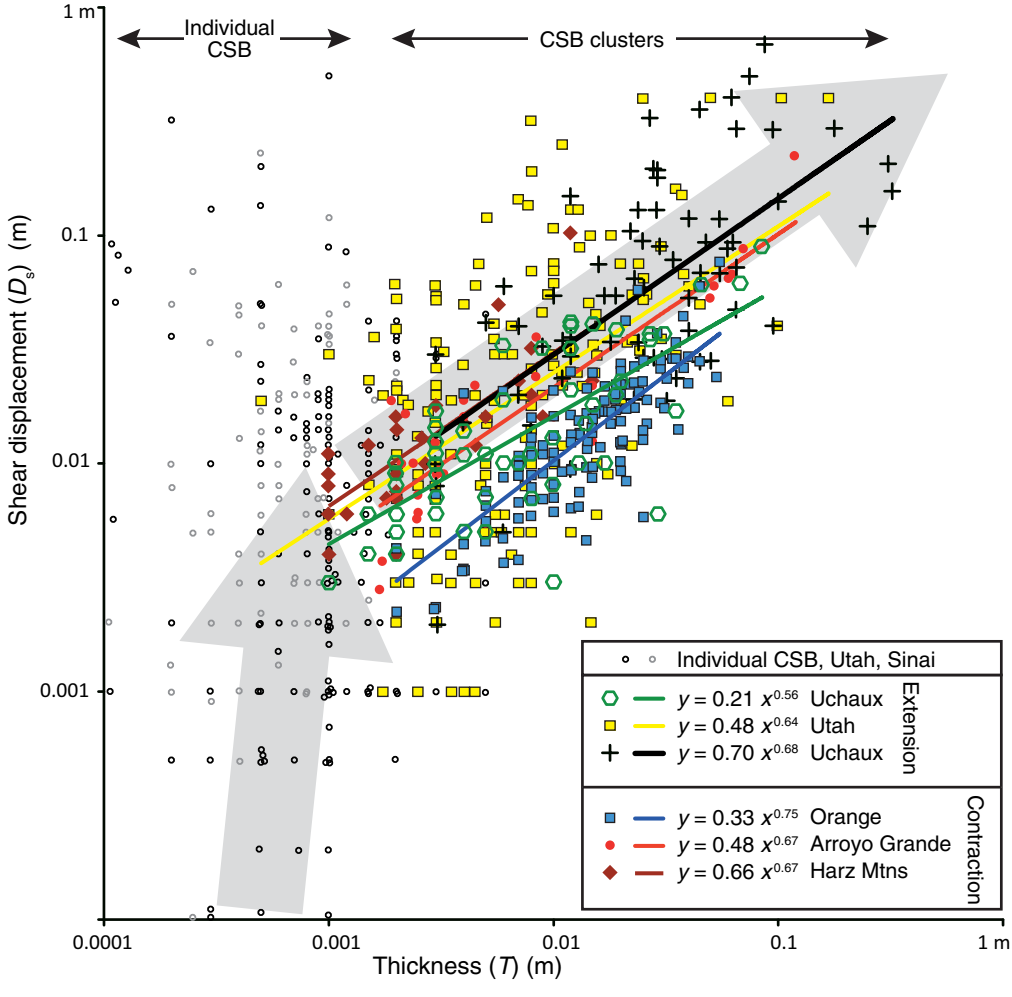

Fig. 3. Thickness of compactional shear bands (CSB) and clusters of CSB plotted against displacement for well-constrained datasets from localities Uchaux and Orange, Provence (France; see Soliva *et al.* 2013 for locations), Utah (Entrada Sandstone, San Rafael Desert, area described in Johansen & Fossen 2008), Arroyo Grande, California (site described by Antonellini *et al.* 1999), Sinai (Rotevatn *et al.* 2008) and Hartz Mountains, Germany (see Klimczak & Schultz 2013). Grey arrows suggest the general growth trend, which changes from almost constant thickness growth of individual bands (vertical arrow) to constantly thickening clusters. Data from Ballas *et al.* (2012), Soliva *et al.* (2013), Johansen & Fossen (unpublished) and own unpublished data.

process the cluster thickens and compacts as shear displacement accumulates; during the evolution of clusters there is therefore a positive correlation between thickness and displacement (Fig. 3). In order to examine the relation between zone thickness (T) and shear displacement (D_s), data from CSB clusters from different tectonic settings and burial depths were compiled and presented in Figure 3. This figure shows a remarkably similar power-law relationship between D_s and T for all the datasets, with an exponent around 0.6–0.7, meaning that T grows faster than D_s as the clusters evolve at the form $D_s = aT^{0.65}$, where a is a constant.

The ratio between shear and compaction displacement (S/C) for all deformation band types is plotted in Figure 4, and is seen to vary considerably. For the classical CSB found on the Colorado Plateau (Utah) and in Sinai, the S/C ratio is very high (>100 for well-developed bands). A much larger variability is seen for CSB from Provence, with S/C values ranging from >100 to 4. We suspect that this

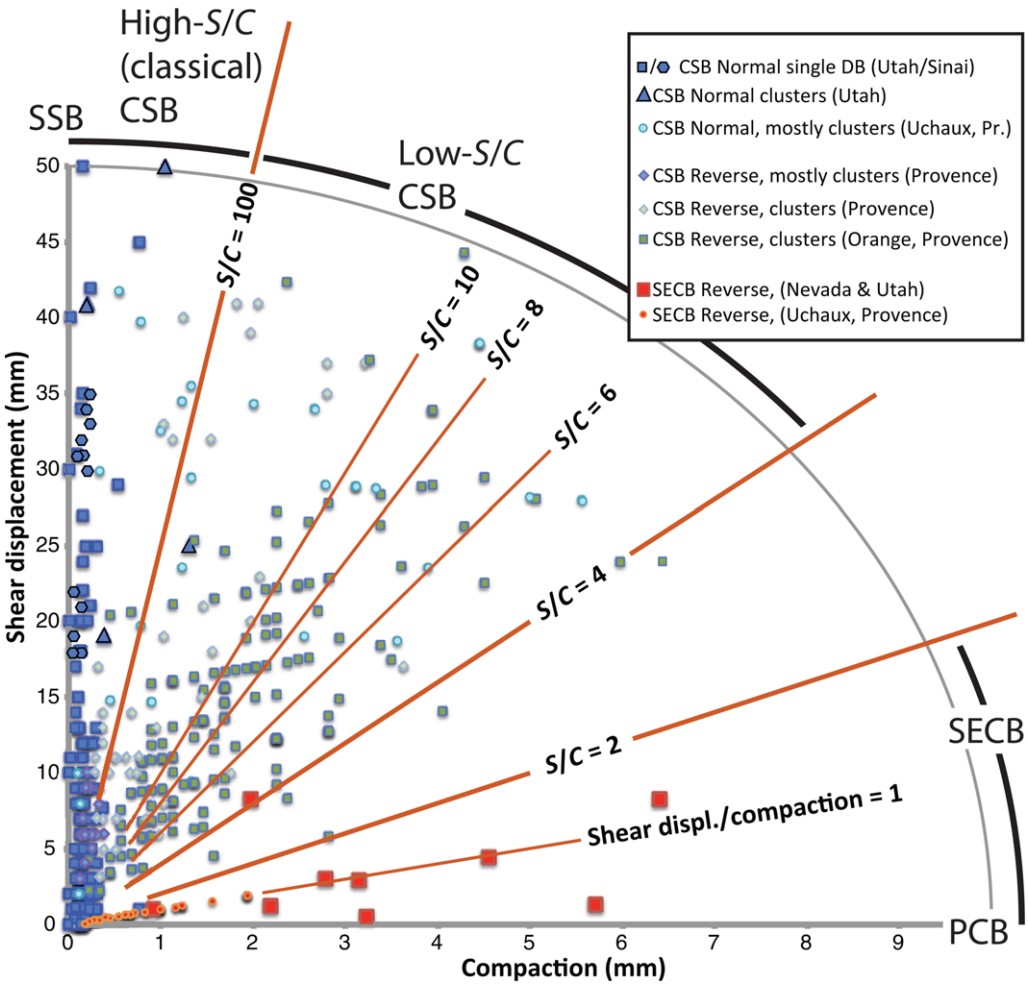

Fig. 4. Band-perpendicular shortening (compaction) plotted against shear displacment. Shear-enhanced compaction bands (SECB) plot in the lower part of the diagram, close to the S/C=1 line where the contribution of shear and compaction are of similar magnitude. Classical compactional shear bands (CSB) plot in the upper part, while clusters of CSB from Provence (extensional and contractional) plot in a wider sector of the upper diagram. Acronyms as for Figure 2.

variability may be related to their poorer compaction and lower confining stress due to shallower burial depths ($\leq$500 m as compared to 2–3 km for the Colorado Plateau bands).

Deformation bands that show much smaller amounts of shear offset ($S/C < 2$; Fig. 4) than the CSB described above have relatively recently been recognized, and are named shear-enhanced compaction bands (SECB) (Eichhubl *et al.* 2010). These bands are usually thicker, up to several centimetres (Fig. 5a, b), show less intense cataclasis, and tend to form conjugate sets (Fig. 5e). Their shear offsets are at the millimetre scale and may be difficult to discern, which has led some authors to classify them as (pure) compaction bands (e.g. Sternlof *et al.* 2005). However, the fact that they arrange themselves into conjugate sets similar to CSB and shear fractures suggests that they involve a small component of shear; they plot close to the $S/C = 1$ line in Figure 4, where the components of displacement from shear and compaction are similar. So far, SECB have only been described from the contractional regime, more specifically from sandstones deformed during the Sevier orogeny in Nevada (Eichhubl *et al.* 2010; Fossen *et al.* 2015), the Laramide orogeny in southern Utah (Schultz 2009; Schultz *et al.* 2010; Fossen *et al.* 2011) and the Pyrenean orogeny in southern France (Ballas *et al.* 2013).

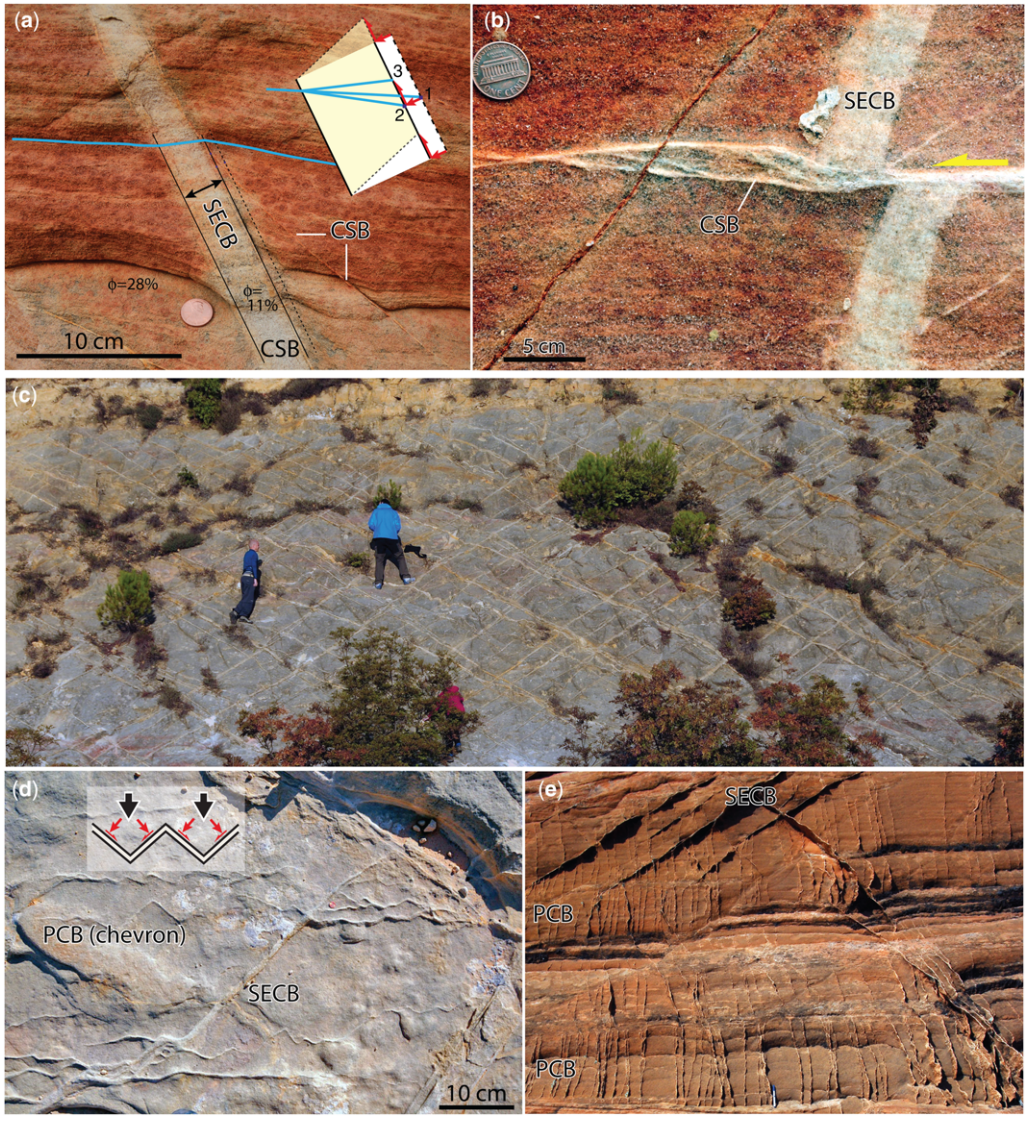

Fig. 5. Examples of deformation bands in the contractional regime. (**a**) SECB 2.5 cm thick and with a slight shear influence on the lamination. (**b**) SECB cut by thin cluster of CSBs. (**c**) Network of CSB clusters (thin) with reverse offsets, Orange, Provence, France. (**d**) Chevron-type PCBs together with SECB. Note how they transition from one type to the other. Inset shows a simple kinematic model, where each 'limb' is acting as a SECB. Black arrows represent the shortening direction. (**e**) Wiggly PCB (vertical) in highly porous (25–30%) sandstone layers and conjugate set of SECB in somewhat less porous layers, Buckskin Gulch, Utah.

Similarly, pure compaction bands (PCB) (Fig. 5d, e) are structures that have only been found in sandstone with very high porosity and are only associated with contractional deformation (Mollema & Antonellini 1996; Schultz 2009; Eichhubl *et al.* 2010; Schultz *et al.* 2010; Fossen *et al.* 2011, 2015). These structures plot along the horizontal axis of Figure 4 and most of them can be sorted into two types: a chevron-style PCB type with a zig-zag geometry (Fig. 5d) where each chevron element ('limb') can be considered to be a SECB, as illustrated in Figure 5d; and a wiggly or undulating type where the undulations are at a smaller scale and more sinusoidal (Fig. 5e). The latter type bears geometrical as well as kinematic similarities to stylolites. The chevron type has a wavelength of

5–10 cm and band thickness of 1–3 cm, while the wiggly type are thinner (millimetre thickness) and with a *c.* 0.5 cm wavelength. In some cases PCB can become close to planar (Liu *et al.* 2016). All types of PCB bisect the obtuse angle between contemporaneous SECB or CSB (Fig. 5e), and form perpendicular to the principal shortening direction. For the minute strains represented by these structures, the principal shortening direction closely corresponds to the local maximum principal stress direction (σ_1) in most cases.

In addition to the bands described above, dilation bands have been reported from unconsolidated sand (Du Bernard *et al.* 2002) and are thought to have formed at shallow depths. Dilation bands have higher porosity than their host rock, unless secondary mineral growth has occurred. Bands with higher internal porosity than their host rock have also been observed in the Nubian Sandstone in Sinai (Fossen *et al.* 2007, fig. 8a), but it is unclear if this increase in porosity is due to later removal of material by fluids.

Conditions controlling deformation band mechanisms

The different kinds of bands described above form according to local stress conditions and to variations in rock properties and characteristics, several of which are directly or indirectly related to burial depth. The most important of these conditions and properties will be briefly discussed here (see Fig. 6 for an overview).

In a simplistic framework, deformation of unconsolidated sand or poorly consolidated sandstones at shallow depths (less than *c.* 200 m) promotes simple shear kinematics, non-cataclastic deformation and, in some cases, also pure compaction and dilation. Important factors in this context are the low levels of stress from the overburden, fluid (over)-pressure, mineralogy and cementation. In granular media, stress is transmitted across grain-to-grain contacts, and low stress across such contacts allows for grain disaggregation. Hence, the fact that stress related to overburden is low at shallow burial depths implies that grains can more easily move relative to one another, while the higher stress at deeper burial depths promotes cataclasis. However, overpressure counteracts the effect of burial and reduces the effective stress so that disaggregation (non-cataclastic flow) can occur at deeper depths. In some cases overpressure can also make the minimum stress negative and thus promote the formation of dilation bands.

In addition to burial depth and overpressure, grain rounding and sorting influence the stress level at grain contacts: the smaller and fewer the grain-to-grain contacts, the higher the stress across each interface. Since well-rounded grains display smaller contact surfaces and since good sorting creates fewer contact points, both favour cataclasis (Cheung *et al.* 2012). This can be seen in the field where bands cross sandstone layers of different sorting, such as the aeolian Entrada Sandstone on the Colorado Plateau; bands are strongly cataclastic in coarser and better-sorted aeolian dune layers and transform into bands with less cataclasis in more poorly sorted and more fine-grained interdune units (Fossen & Gabrielsen 2005, p. 130).

Mineralogy is important because different minerals have different strengths. Carbonate clasts are

Variable	Granular flow → Cataclasis
Burial depth (confining stress)	Shallow → Deep
Lithification	Unconsolidated → Well lithified
Fluid overpressure	High → Low
Cement strength	FeO(OH) (low) → $CaCO_3$ → SiO_2 (high)
Grain roundness	Angular → Rounded
Grain sorting	Poor → Good
Mineralogy (grain strength)	Strong → Weak
Phyllosilicate content	High → None
Tectonic regime	Extensional → Contractional

Fig. 6. Factors influencing the degree of cataclasis in deformation bands.

weaker than feldspar, which are again weaker than quartz grains. Deformation bands in unconsolidated carbonates may therefore show fractured carbonate clasts even when deformed very close to the surface. Similarly, feldspathic arenites can also show grain fracturing at relatively shallow depths (<1 km), as demonstrated in poorly lithified Tertiary arenites from the Rio Grande rift, where feldspar cleavage was found to be activated as microfracture surfaces, together with the fracture of lithic fragments, while quartz grains were largely devoid of transgranular microfractures (Rawling & Goodwin 2003). These authors also recognized that while the quartz rarely developed transgranular fractures, small flakes of quartz were chopped off some of the quartz grains ('flaking'). In addition to mechanically weak minerals, platy minerals (phyllosilicates) can have a lubricating effect on grain boundaries, favouring non-cataclastic granular flow. They may also rearrange themselves to form a band-parallel fabric that reduces fluid flow across the deformation bands, commonly referred to as phyllosilicate bands (Knipe *et al.* 1997; Fossen *et al.* 2007). Phyllosilicate bands are common in sandstone reservoirs of the North Sea Jurassic, where mica- and clay-bearing sandstones were deformed at relatively shallow depths (0–1 km) shortly after deposition (see Fisher & Knipe 2001); these are not discussed in detail in this work.

Tectonic stress alters the state of stress generated by the overburden. In the extensional regime, the minimum horizontal stress (σ_3) is reduced and hence reduces the likelihood of grain fracture at shallow levels. In simple terms, the effect is that grains can more easily move in the horizontal direction without breaking (non-cataclastic granular flow). For the contractional regime the effect is the opposite: the mean stress increases as the tectonic stress adds to the horizontal stress (Soliva *et al.* 2013). We may therefore expect cataclasis to occur at shallower depths in the contractional than in the extensional regime. This may be an important reason why reverse cataclastic deformation bands occur in poorly consolidated quartz sands in Provence that have not been buried below *c.* 500 m (Ballas *et al.* 2014). However, in this area, cataclastic deformation bands also developed during a later extensional phase of deformation, which is unusual for such low burial depths. One explanation may be that the contraction phase caused an additional overall compaction of the sands, and that this additional compaction may have changed the material properties enough to utilize cataclasis during the extension (Wibberley *et al.* 2007).

It is clear that many factors influence the deformation mechanisms of deformation bands (Figs 6 & 7). Nevertheless, cataclasis is more commonly observed in sandstones that underwent deformation at depths deeper than 1–1.5 km, and may therefore be expected to have obtained some degree of lithification through compaction and cementation/dissolution. When analysing or predicting deformation band formation it is important to consider the rock properties at the time of deformation, which may have been quite different from the present state. Timing of deformation relative to the burial/uplift history and related lithification history of the sedimentary rock is equally important. This is why sandstones typically show several distinctly different sets of structures, such as early soft-sediment structures and/or disaggregation bands formed at shallow levels, overprinted by cataclastic CSB formed at deeper levels, and finally late joints if the sandstone has been exhumed.

Deformation bands in the extensional regime

Deformation bands were first explored in the extensional regime, where they tend to accumulate in zones or clusters (Soliva *et al.* 2016). This strong tendency of localization is particularly pronounced for cataclastic normal-offset deformation bands, but is also observed for many non-cataclastic (disaggregation) bands of tectonic origin, for instance from the Jurassic siliciclastics of the North Sea rift (Hesthammer & Fossen 2001). Exceptions are disaggregation bands (simple shear bands) related to non-tectonic soft-sediment deformation, such as soft-sediment folding, diapirism and gravity sliding. The distribution of such bands is controlled by the kinematics of the larger-scale deformation process.

Fault precursors

It is well documented from several field studies that faults in porous sandstones form in or along deformation band zones (clusters) that grew from single deformation bands (Aydin & Johnson 1983; Shipton & Cowie 2001). Hence, as precursors, deformation band zones dictate or strongly influence the location and orientation of faults. Fault formation occurs by the establishment of a slip surface or fault core where offsets are much larger than those accumulated by deformation bands and deformation band clusters. In addition, transitional stages from deformation band clusters with incipient and discontinuous slip surfaces to those with a continuous slip surface can be observed.

The point at which the through-going slip surface develops is quite variable between different rock units. Some units, such as the Navajo Sandstone in Utah, can display very thick CSB clusters, locally consisting of hundreds of bands in a several-decimetres-thick zone developed prior to

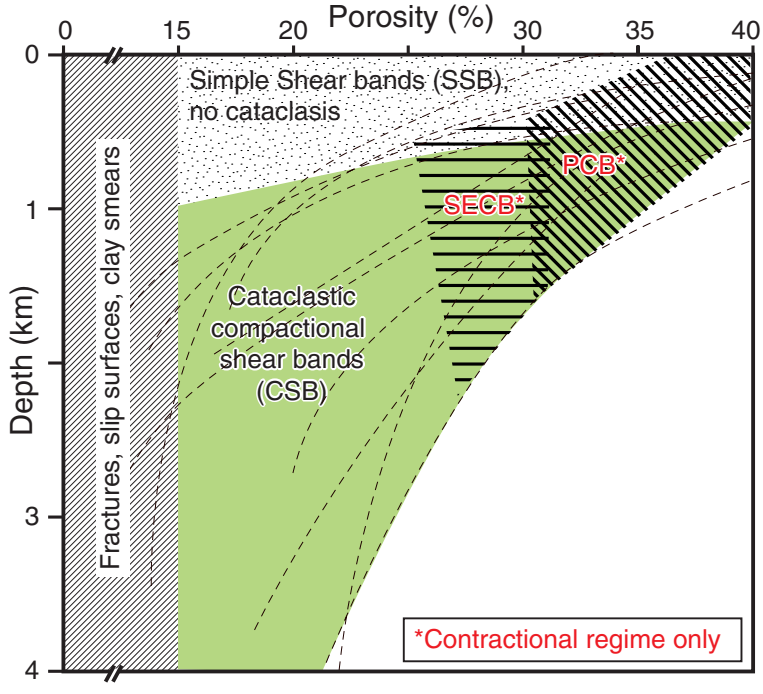

Fig. 7. Depth-porosity diagram tentatively showing the fields where different types of deformation bands are commonly observed to form in porous siliciclastic rocks. Porosity–depth curves for sandstones from Rieke & Chilingarian (1974, p. 42) are indicated by dashed lines.

faulting. Most other sandstones develop thinner clusters prior to faulting, and a good understanding of the controlling factor(s) is yet to be achieved. A clear example from the San Rafael Desert (Utah) of how clusters vary in thickness with respect to lithological variations is shown in Figure 1b, where the thickness of the CSB cluster increases systematically upwards as it moves from very fine-grained to coarser-grained and more porous Entrada Sandstone. Grain-size observations and permeability values obtained with a portable micropermeameter (TinyPerm II) were collected from the host rock at this and several neighbouring outcrops, and the results (Fig. 8b, c) show clear connections among host-rock grain size, permeability and CSB cluster thickness. Data from three cluster zones at different stages of maturity are shown, and they all define a similar trend with respect to grain size as indicated by the dashed lines in Figure 8c. The CSB clusters transition into a striated slip surface as the grain size is reduced to 0.2–0.1 mm and as permeability is decreased to around 20 mD (Fig. 8). This corresponds to a critical minimum porosity value of around 15% for deformation band formation (porosity estimated from thin-sections) which, considering the very low degree of cementation and dissolution in this sandstone, is expected to be close to the actual porosity at the time of deformation. Where these cluster zones develop further, they eventually display a slip surface along the entire zone, typically at a thickness of around 10–20 cm at this particular site. Clearly, this variability in thickness with respect to lithology is responsible for some of the scatter seen in T–D plots (Fig. 3), together with the lateral variations within layers (Fossen & Bale 2007).

The damage zone

As a fault is established in porous sandstone, by definition the surrounding precursory deformation bands become the fault damage zone. Investigations of damage zones from a number of faults with a variety of offsets show a positive non-linear relationship between fault displacement and damage zone thickness corresponding to a power-law ($T = aD^b$) with exponent b close to 0.5 (Fig. 9), and with a statistically slightly thicker damage zone in the hanging wall (Schueller *et al.* 2013). In other words, the damage zone grows in thickness as the fault accumulates displacement. However, there is a significant variation in damage zone thickness for any given fault displacement (Fig. 9) which depends on a number of factors, such as fault growth

history (extent and nature of fault linkage in both the horizontal and vertical directions), fault geometry, fault core strength and the nature of the host rock.

Even if damage zones grow in thickness as new deformation bands form around the fault core, data from normal faults in porous sandstones studied by Schueller *et al.* (2013) show that the average density of bands (15 ± 9 bands/m) is statistically independent of fault displacement. Also, the distribution of bands within the zone is qualitatively similar for small and large faults. Field-based observations consistently show that the highest densities of deformation bands occur close to the fault core, with a fall-off in deformation band density towards the margin of the damage zone. Although there is a significant quantitative variation in how the deformation bands are distributed within the damage zone, data from highly porous sandstones in Utah and Sinai show that most band distributions in such lithologies are best modelled by a logarithmic function of the form $Y = A + L\ln(X)$, where Y represents the number of deformation bands per metre and X the distance from the fault core (Schueller *et al.* 2013) (Fig. 10).

In detail, the bands in the damage zone tend to cluster which creates local deviations from the smooth logarithmic model shown in Figure 10. The clusters are thicker with more internal bands close to the fault core (Johansen & Fossen 2008), and it is clear that clusters develop into thicker and denser zones in coarser-grained sandstone relative to finer-grained lithologies. Statistical analysis of damage zones in porous sandstones indicates that the degree of clustering is independent of fault displacement, so that the clustering patterns are similar throughout the fault growth history (Du Bernard *et al.* 2002; Schueller *et al.* 2013).

Based on these findings, the damage zone can be considered to grow from an initial process zone with a constant balance between the formation of new deformation bands in the existing damage zone and the creation of new bands outside (Fig. 11). Moreover, as the width of the damage zone increases throughout the active lifetime of a fault, the distribution of deformation bands in the damage zone remains self-similar. Both band distribution and damage zone width for seismically mapped faults can therefore be modelled from the relationships shown in Figures 9 and 10.

Conjugate sets of deformation bands

A very characteristic feature of compactional shear band (CSB) populations in the extensional regime is the formation of conjugate sets of bands or band clusters, that is, sets dipping in opposite directions and mutually cross-cutting each other (Fig. 1d) (Chemenda *et al.* 2014). Conjugate deformation band populations are in many places bimodal, consisting of only two sets and therefore consistent with plane strain, although in detail they tend to display a range in orientation and a certain non-planarity of the bands and band clusters (Fig. 1d).

In cases where the variation in orientation is significant the bands form a polymodal or orthorhombic pattern, consistent with non-plane or 3D strain (Underhill & Woodcock 1987; Healy *et al.* 2015). The Goblin Valley area in the San Rafael Desert, Utah is interesting in this sense. Here an array of small ($<$20 m displacement) normal faults generated from deformation band zones are fairly straight and parallel in map view, and hence consistent with overall plane strain. However, locally we see that the faults change orientation where they link, and these are sites of a larger range in deformation band orientation. As an example, a site of fault interaction in the Goblin Valley area has been mapped in detail, as shown in Figure 12. This site exhibits bands with a considerable range in orientation and oblique-slip fault kinematics, that is, not consistent with a bimodal plane strain situation.

We also observe outcrop-scale deviations from simple conjugate sets due to the way that deformation bands perturb the stress field. This is most clearly seen where bands intersect; the band zones tend to split up into strands with somewhat different orientations (e.g. Fig. 1d; Aydin & Reches 1982; Fossen *et al.* 2005). It is therefore possible that deviations from the perfect conjugate situation in some cases may be related to local variations in the stress field during fault and band interaction, with the large-scale strain field still being close to plane strain. Polymodal deformation band populations may therefore, but do not have to, indicate regional non-plane strain.

Conjugate sets ideally form with *c.* 60° dihedral angles according to the Mohr–Coulomb theory of faulting. Natural deformation bands and band clusters show quite a wide range in orientation of the dihedral angle however, mostly over 35–95° in the extensional regime (Fig. 13). Most conjugate sets of CSB define angles in the range 35–67° for the extensional regime (47° example shown in Fig. 1d). The small dihedral angles observed for some CSB (Fig. 13) (e.g. Underhill & Woodcock 1987; Johansen & Fossen 2008) are difficult to explain. Hybrid shear fractures that involve a combination of shear and positive dilation tend to form dihedral angles $<$60° (Hancock 1985), but CSB involve a combination of shear and compaction (negative dilation). Overall, it is likely that the angles are related to the initial properties (friction and dilation angles) of the host rock, the initial properties of the bands, and how these properties evolved with the stress state during the process of shear and volumetric deformation.

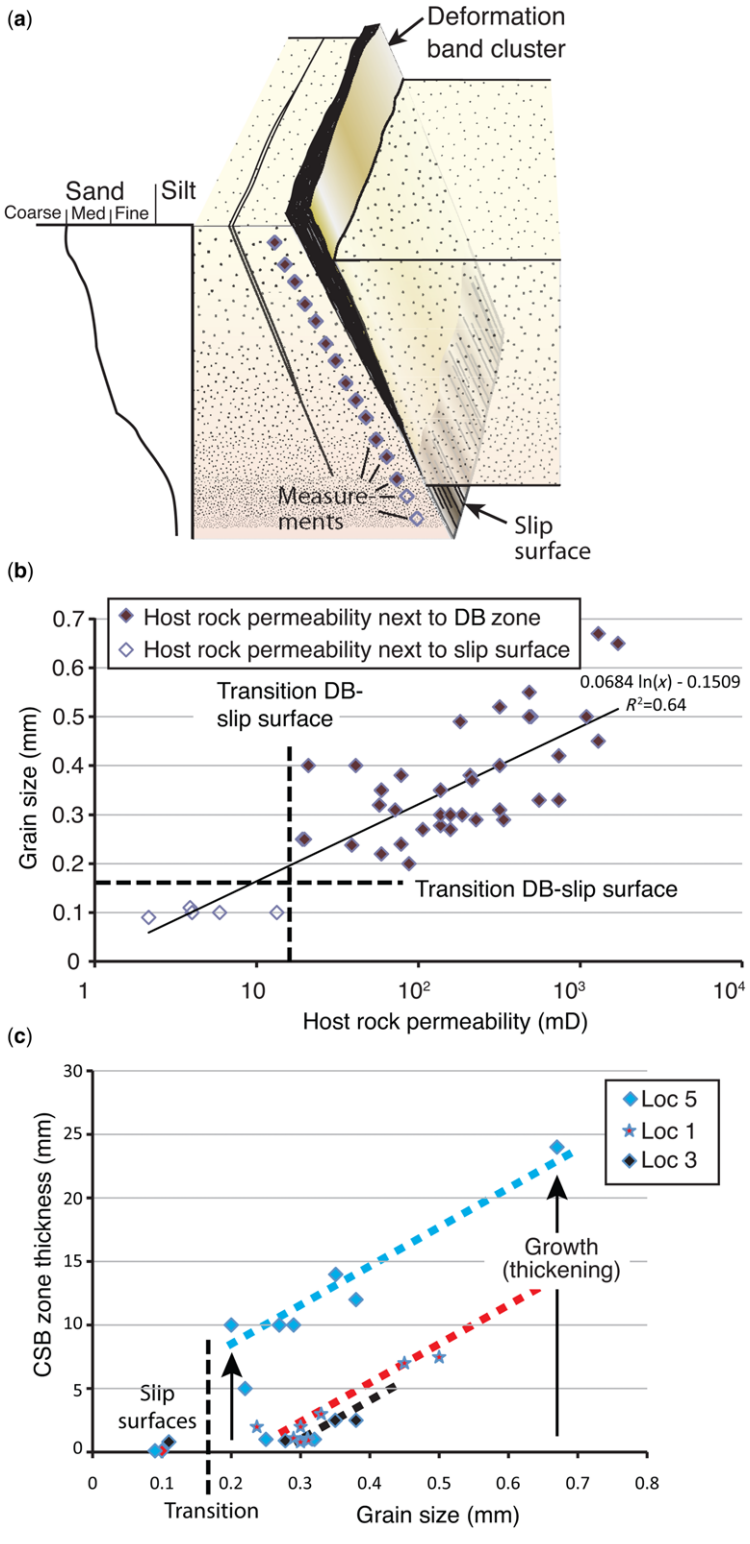

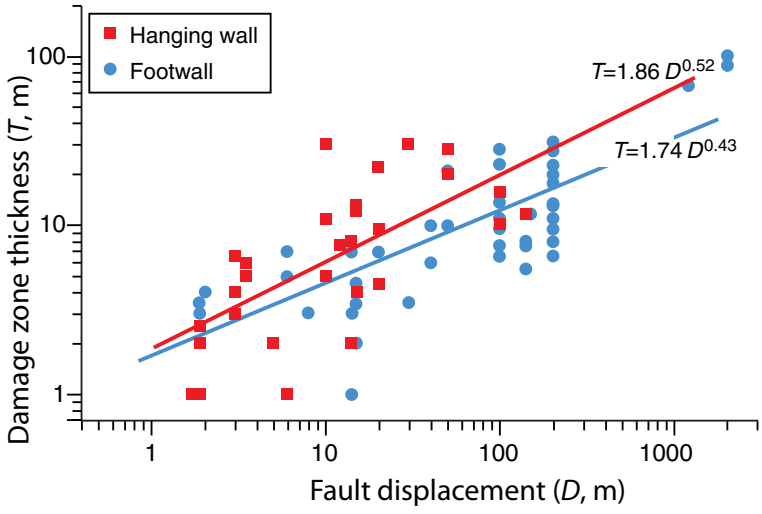

Fig. 9. The relationship between fault displacement and damage zone thickness for porous sandstones can be modelled with an exponential function with an exponent around 0.5. From Schueller *et al.* (2013).

Deformation bands in the contractional regime

Observations of deformation bands in the contractional regime are more limited than for the extensional regime, with the best-studied areas being the Valley of Fire/Muddy Mountains area in Nevada (the Jurassic Aztec Sandstone), southernmost Utah (Buckskin Gulch; Jurassic Navajo Sandstone) and Provence, France (Upper Cretaceous sands of the South-East Basin). In these places, deformation bands appear more evenly distributed than those observed in the extensional regime in the same or similar rock units (Soliva *et al.* 2016), particularly where thrusting and layer-parallel shortening are involved. Several recent papers describe arrays of broadly distributed SECB and CSB in poorly lithified Cretaceous sandstones in Provence (Klimczak *et al.* 2011; Soliva *et al.* 2013). The pre-faulting localization of deformation bands into zones that characterize the extensional regime is not observed here. Instead, cataclastic bands or thin clusters form two sets of oppositely dipping conjugate CSB structures, both of which developed during the Pyrenean phase of N–S contraction (thrusting and folding). Very similar patterns are seen in Arroyo Grande, California (Antonellini *et al.* 1999).

SECB also form conjugate sets in the most porous strata of the Provence sandstones and, although the two sets are seen to cross each other, they more commonly alternate along the strata. This characteristic occurrence is also seen in the Aztec Sandstone in the Valley of Fire/Muddy Mountains area and in the Navajo Sandstone in southern Utah. The spacing of the SECB is larger for these US examples (typically *c.* 0.3 m) than in Provence (a few centimetres), with no obvious relationship to mechanical layer thickness. The contrast in elastic stiffness between the different sandstone layers constituting the sandstone and the friction between them seem responsible for these differences of band spacing and organization (Chemenda *et al.* 2014).

PCB only occur in the most porous layers, and have only been observed in aeolian sandstones in the abovementioned localities in the US. Similar to SECB, they do not develop distinct clusters but distribute themselves along layers with sufficiently high porosities. The millimetre-thick wiggly bands typically occur as individual structures or as

Fig. 8. (**a**) Field sketch and (**b**) plot of host-rock permeability against grain size for the Entrada Sandstone in a few neighbouring outcrops in the San Rafael Desert. Permeability and grain size were measured in the host rock along the deformation band zone (cluster) together with the zone thickness. Filled symbols are deformation bands (CSB) while open symbols represent slip surfaces in fine-grained sandstone. The data show that CSB transition into slip surfaces at grain sizes 0.1–0.2 mm and permeability values around 20 mD. Grain size was estimated from thin-sections and high-resolution macro-lens field photos. (**c**) CSB cluster thickness plotted against grain size for three structures, quantifying how the clusters systematically grow thicker in the coarse-grained sandstones relative to the finer sandstones.

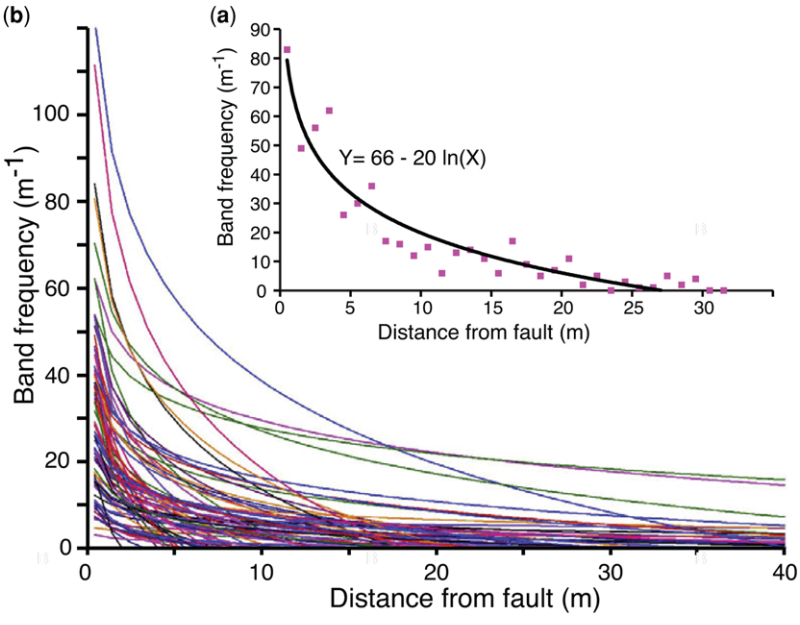

Fig. 10. (**a**) An example of CSB density reduction away from fault core (origin) and how a logarithmic function can be fitted to the data, Entrada Sst, Moab fault system. (**b**) Multiple logarithmic curves from more than 100 damage zones from porous sandstones in Utah and Sinai, as presented by Schueller *et al.* (2013).

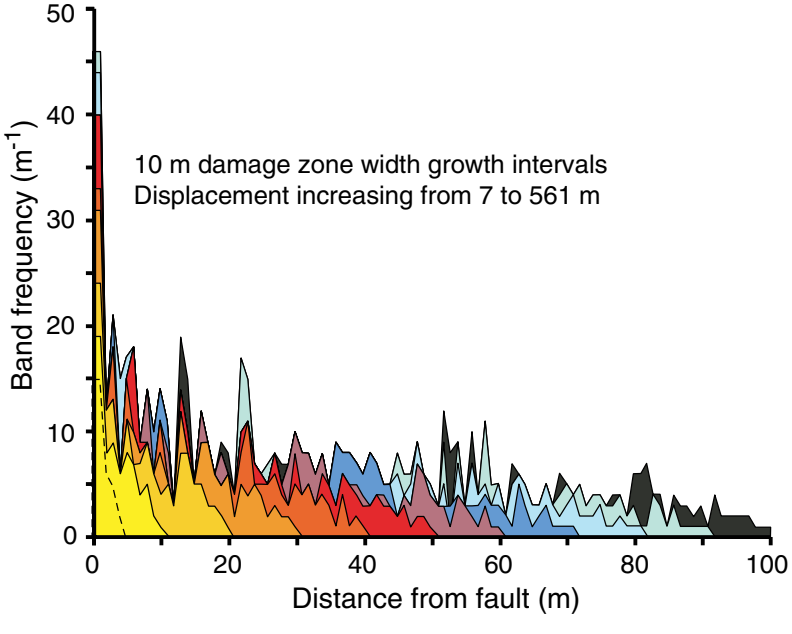

Fig. 11. Simulated damage zone growth from a probabilistic model based on data shown in Figures 9 and 10 (see Schueller *et al.* 2013 for details). The displacement for each step (arbitrarily coloured) increases from an initial 7 m displacement to 103 m for the last step. The 'statistical growth' of the damage zone is characterized by the creation of new deformation bands both within and outside the existing damage zone.

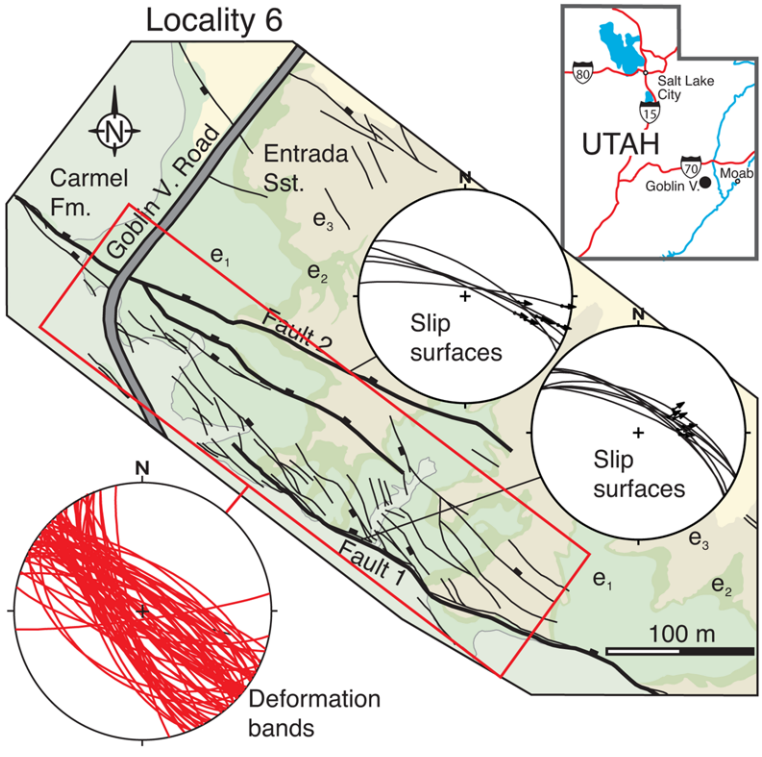

Fig. 12. Structural map of a site of fault tip interaction in the San Rafael Desert near Goblin Valley (Loc. 6 in Johansen & Fossen 2008). Spherical projection of deformation band orientations (lower-hemisphere projection) show a range of orientations (polymodal) with an average NW–SE strike and dip directions ranging from NE through vertical to SW.

structures with up to a few strands that show a spacing that relate closely to the permeability and porosity of the host rock: the higher the porosity and permeability of the layer, the higher the PCB density (Fig. 14).

Conjugate sets

As already mentioned, deformation bands in the contractional regime also form conjugate sets, but with a different range of dihedral angles. Conjugate sets of SECB consistently define high dihedral angles (70–100°) (Fig. 13), well above the *c.* 60° dihedral angles predicted by to the Mohr–Coulomb theory of faulting. In contrast, conjugate sets of CSB in the contractional regime show angles in the range 40–75°.

High dihedral angles for SECB sets were also reported by Eichhubl *et al.* (2010), some as high as 106°. It is tempting to relate the high dihedral angles of SECB to kinematics: the higher the S/C ratio (Fig. 4), the higher the dihedral angle. For PCB, which only involve compaction (S/C being infinitely small), the dihedral angle is 180°, that is, the two conjugate sets collapse to define one set that is perpendicular to σ_1. However, a continuous transition is generally not seen as there seems to be a jump between conjugate planar SECB with dihedral angles $<106°$ and non-planar PCB forming just a single set of bands. However, the transition from SECB to CSB seems somewhat more gradual in terms of both S/C ratio (Fig. 4) and dihedral angle (Fig. 13).

Why SECB and PCB are limited to the contractional regime

Empirical evidence indicates that PCB and SECB, that is, bands with only compaction displacement or where compaction and shear are of similar magnitude, form at conditions where the effective mean stress (confining pressure) p is high relative to the differential stress q. The contractional regime involves the addition of a positive (compressional) horizontal tectonic stress, while the extensional regime is associated with a reduction in the horizontal stress (Wibberley *et al.* 2007; Soliva *et al.* 2013).

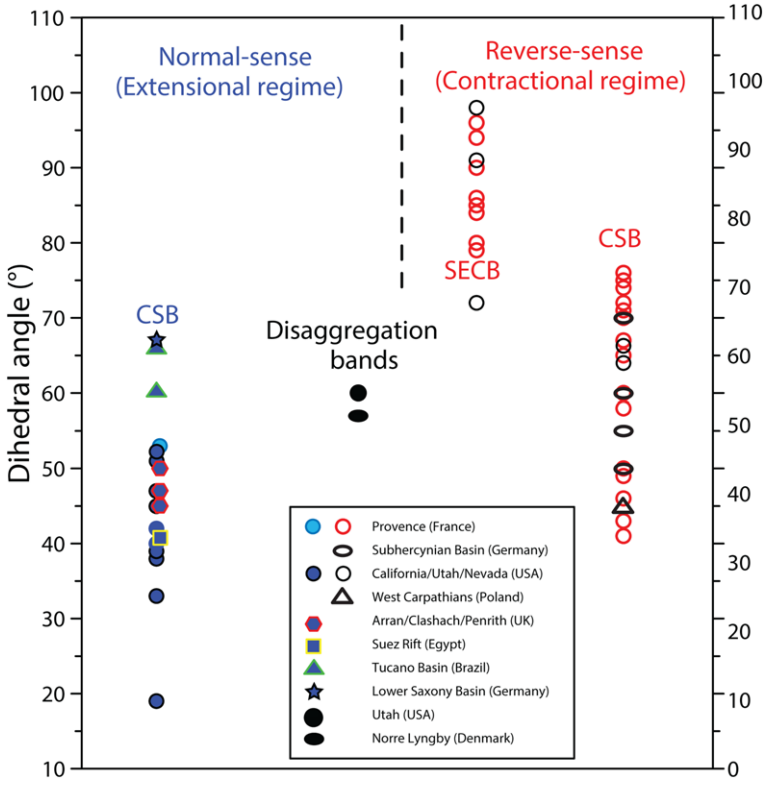

Fig. 13. Dihedral angle of conjugate deformation bands of various types, separated by tectonic regime.

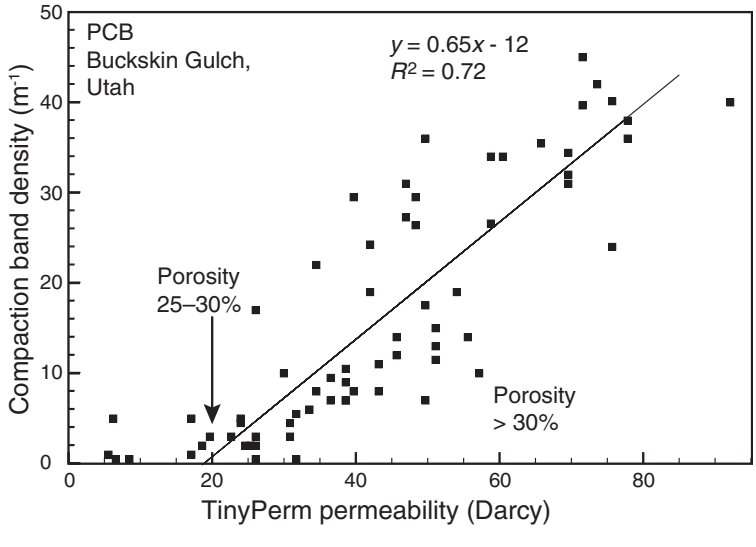

Fig. 14. Diagram showing how the density (spacing) of PCB in the Navajo Sandstone in southern Utah increases with increasing host-rock permeability as measured by the TinyPerm II minipermeameter (note that TinyPerm values are higher than regular He plug measurements by a factor of *c.* 1.8). Porosity is >25% where PCB exist, probably increasing to the right in the diagram (no data in the most porous and friable parts of the sandstone). See Fossen *et al.* (2011) for more information.

This difference implies that the stress paths for a sand or sandstone are different for the two tectonic regimes, as illustrated in the $q-p$ diagram in Figure 15, where the tectonic stress is applied at point (1). The $q-p$ diagram is commonly used to represent the state of stress and mode of deformation of granular materials (e.g. Antonellini *et al.* 1994; Schultz & Siddharthan 2005; Soliva *et al.* 2013) and contains an approximately linear envelope for frictional sliding (critical state line), and an elliptical envelope (cap) for compactional flow. Permanent deformation (plastic yielding) occurs when the stress path intersects the yield cap or the critical state line.

Experimental work shows that the cap has an elliptical shape (e.g. Zhang *et al.* 1990; Wong *et al.* 1997; Grueschow & Rudnicki 2005) and that its intersection P^* with the horizontal p-axis depends on the grain radius R and porosity ϕ through the approximate relationship $P^* = (\phi\ R)^{1.5}$. The position of the cap in the $q-p$ diagram is therefore defined by the local lithology (grain size and porosity), whereas the stress path is controlled by the amount of overburden (burial depth) and tectonic stress. Furthermore, the mode of deformation at the onset of permanent deformation is prescribed by the point at which the stress path intersects the cap (e.g. Schultz & Siddharthan 2005; Wibberley *et al.* 2007), and is compactional (PCB and SECB) in the middle part of the cap and shear-dominated (CSB) near the intersection between the cap and the critical state line. As demonstrated by Soliva *et al.* (2013), the expected stress path for a buried sandstone deformed in the contractional (or thrust) regime is one that reaches the yield cap in its central part, where SECB and PCB bands are expected. In contrast, the extensional (normal fault) regime predicts a point of intersection higher on the cap, where shear bands and cataclasis are expected (Fig. 15). According to this simple model, deformation bands forming in the normal regime should therefore be shear-dominated and clustered, while they should be more compactive (SECB and, where porosity is high, PCB) and distributed in the contractional regime, that is, similar to what is generally observed.

The difference in localization between the extensional and contractional regimes is probably related to the amount of shearing involved: numerous studies have documented clustering of shear deformation bands into zones that may or may not evolve into faults or slip surfaces, while contraction, which involves more compaction, result in wider band distributions (Soliva *et al.* 2016). However, CSB that develop in the contractional regime also tend to produce distributed networks (e.g. Fig. 5c). There may also be other conditions (including boundary conditions) that control the distribution of bands.

The impact of boundary conditions and large-scale structures on deformation band populations

The distribution of deformation bands on the hectometre to kilometre scale within a sandstone unit may be viewed as the product of imposed displacement

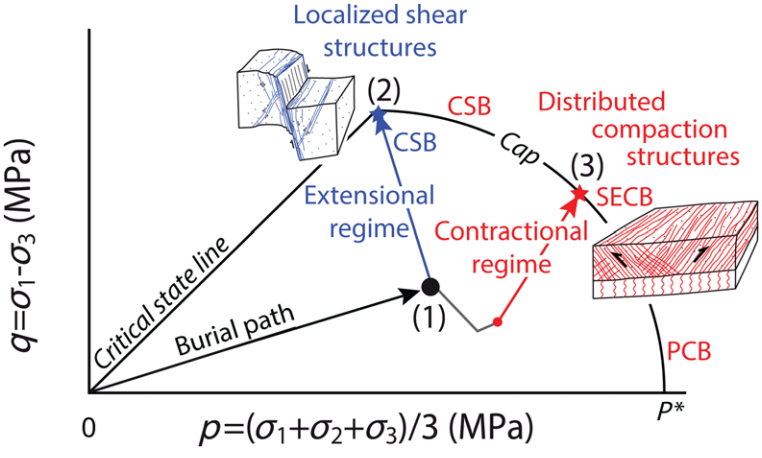

Fig. 15. $q-p$ diagram showing the stress path of a sandstone during burial that at point (1) is exposed to extension, which increases q and reduced p so that the path hits the cap where localized shear bands (CSB) are predicted (2) and contraction, which creates a path that intersects the cap where distributed SECB and PCB are expected (3). See Soliva *et al.* (2013) for details. q: differential stress; p: effective mean stress (confining pressure); P^*: crushing pressure.

or velocity conditions (e.g. Tikoff & Wojtal 1999), which can loosely be referred to as kinematic boundary conditions. From this perspective, stresses and the resulting deformation bands that form in a sandstone body arise from the material response to the imposed velocity and displacement field. In other words, porous sandstone bodies and associated sedimentary layers are generally soft and accommodate strain dictated by movements in underlying units (e.g. basement), overlying units (thrust sheets) and by large-scale structures such as listric faults that impose hanging-wall deformation to a significantly large part of the sandstone unit (Fig. 16j; Fossen & Rotevatn 2012).

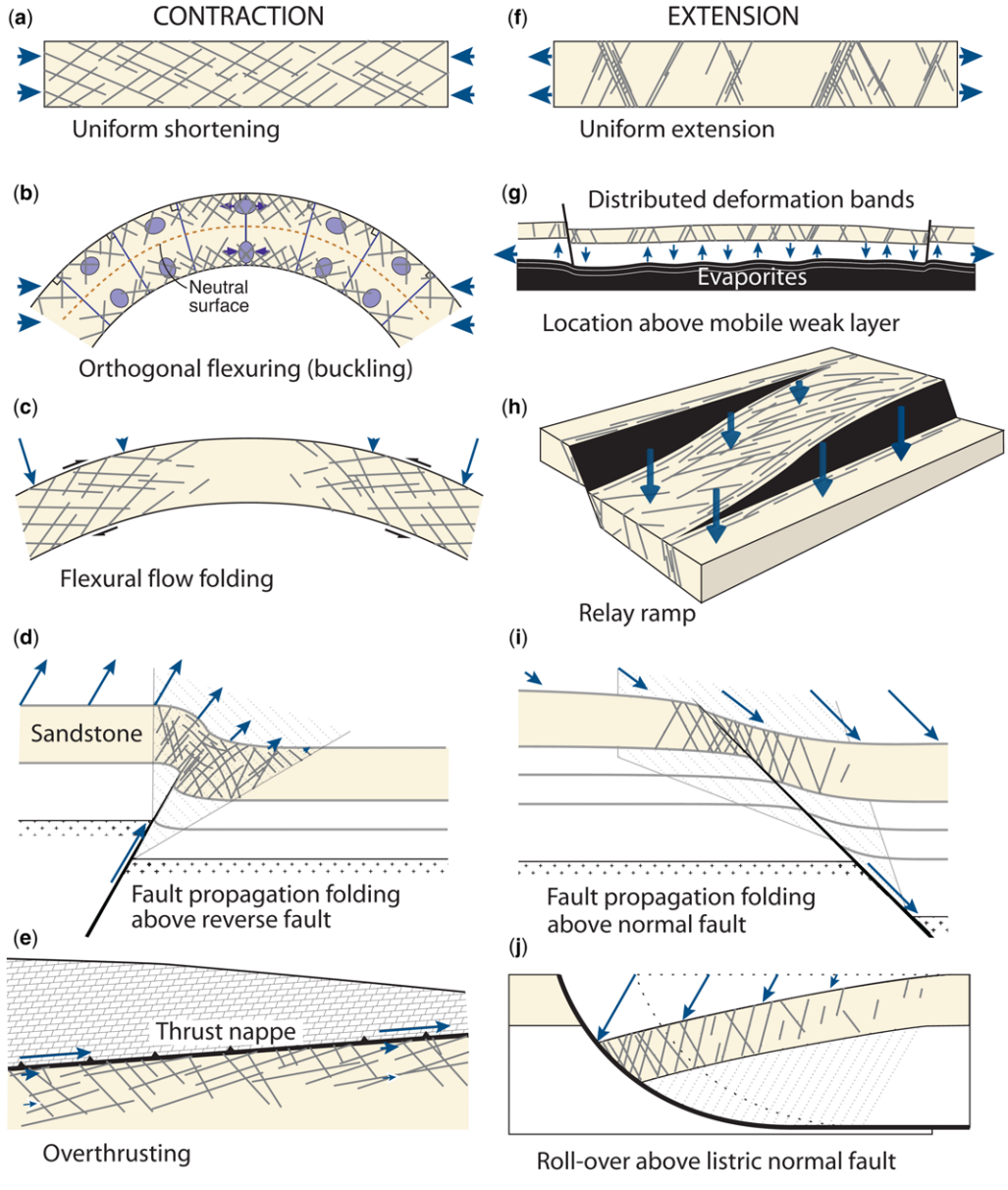

Fig. 16. A series of examples where large-scale structures, most of them external to the sandstone formation in question, control the distribution of deformation bands in the sandstone. In each case the sandstone is 'forced' to deform, and does so by the development of deformation bands if the sandstone is porous enough.

A variety of models are shown in Figure 16 where boundary conditions or large-scale structures can control deformation band distribution. If first-order structural patterns can be mapped and the strain distribution modelled it is possible, particularly with additional information about lithology, to make basic predictions about the orientations, distribution and type of deformation bands. For instance, different fold mechanisms (orthogonal flexure, flexural flow and fault propagation folding) all generate different deformation band populations (Fig. 16b–d, i). Thrust nappe emplacement over highly porous sandstone (Fig. 16e) has been shown to generate populations of SECB and PCB and, after continued compaction, scattered CSB in a wide region underneath the nappe (Fossen *et al.* 2015). Bands are generally more clustered in the extensional regime, but can be widely distributed in large relay ramps (e.g. Rotevatn & Fossen 2011; Fig. 16h) and above mobile soft layers such as shale or salt (Fig. 16g). Large rollover structures (Fig. 16j) can also generate laterally extensive populations of deformation bands, as demonstrated by Antonellini & Aydin (1995) from Cache Valley in Arches National Park, Utah.

Monoclinal structures on the Colorado Plateau, formed by forced folding (fault-propagation folding) in response to reactivation of basement faults, represent excellent examples of how large-scale structures that are seismically mappable can be used to predict deformation band distributions at subseismic scales. The San Rafael monocline in southern Utah is an example from the contractional regime. Here we see a progressive evolution from individual deformation bands to band zones as the fold becomes tighter along-strike, and a relationship between band density and fold tightness (which corresponds to the steepness of the steep limb) can be established (Zuluaga *et al.* 2014). A similar, but somewhat smaller monocline in the Colorado National Monument area (Colorado) shows a similar association, where deformation band density increases towards the steep part of the monocline (Fig. 17). In the two cases the relationship between bed dip and deformation band density is qualitatively similar, but the structural details are different. The San Rafael case shows a gradual evolution from early-stage bedding-parallel CSB to oblique low-angle conjugate (mostly) reverse zones of CSB, while in the Colorado National Monument example bedding-plane bands are somewhat less frequent, and the deformation bands form high-angle extensional conjugate sets. In a very similar monoclinal structure, the Kaibab Monocline (southernmost Utah), PCB and SECB are developed in highly porous sandstone layers (Mollema & Antonellini 1996). These differences can in part be attributed to differences in fold mechanism and/or lithology. Prediction of subseismic deformation bands from large-scale structures can therefore be done in a qualitative way, but should involve site-specific data about physical rock properties.

Deformation bands and fluid flow

Deformation bands of the three types CSB, SECB and PCB all reduce porosity (Fig. 18) and permeability. However, the extent to which deformation bands and related structures influence fluid flow in hydrocarbon reservoirs has been a matter of discussion for several decades (Lewis & Couples 1993; Antonellini *et al.* 1999; Fossen & Bale 2007; Brandenburg *et al.* 2012; Ballas *et al.* 2015). It now seems clear that only very thick clusters of cataclastic deformation bands, particularly if paired with a continuous slip surface (fault), would have the potential to create hydrocarbon traps (Torabi *et al.* 2013). In practice, deformation bands and deformation band clusters both show significant variations in thickness, porosity and permeability, with segments or linkage points that act as points of leakage (Fossen & Bale 2007; Rotevatn *et al.* 2013). As a result, both thickness and segmentation are important controls on fluid flow tortuosity and trap integrity.

A microscale example of a classical CSB from the San Rafael Desert, Utah is shown in Figure 18a, where the porosity in the band is seen to change dramatically on the centimetre-scale. In this figure, pores are shown in blue; the whiter the band, the lower the band porosity. While the original porosity (28%) has been reduced to 1% in the band in region 1 (Fig. 18a), the band porosity is 10% in region 2. Furthermore, the micro-CT-based pore model shows that 90% of the porosity of region 2 is connected, whereas only 60% is connected in region 1 (the host-rock connectivity is close to 100%). Such observations support what has been concluded from theoretical and physical modelling: deformation bands do not have any significant sealing effect (Fossen & Bale 2007; Torabi *et al.* 2013). Cross-cutting joints can also create pathways for fluid flow across deformation bands (Tindall 2006). Nevertheless, deformation bands can introduce a permeability anisotropy to reservoirs (Sternlof *et al.* 2006; Rotevatn *et al.* 2009), and the effect of this anisotropy on fluid flow depends on the extent of their permeability-reducing properties, orientation and distribution.

The reduction in permeability across a cataclastic band is related to the amount of compaction perpendicular to the band walls and, even more so, the amount of band-parallel shear, and is highest for high S/C ratios (upper part of Fig. 4). In most cases, cataclasis is the main control on permeability reduction; the more grain crushing, the lower the porosity and permeability in the band. In other

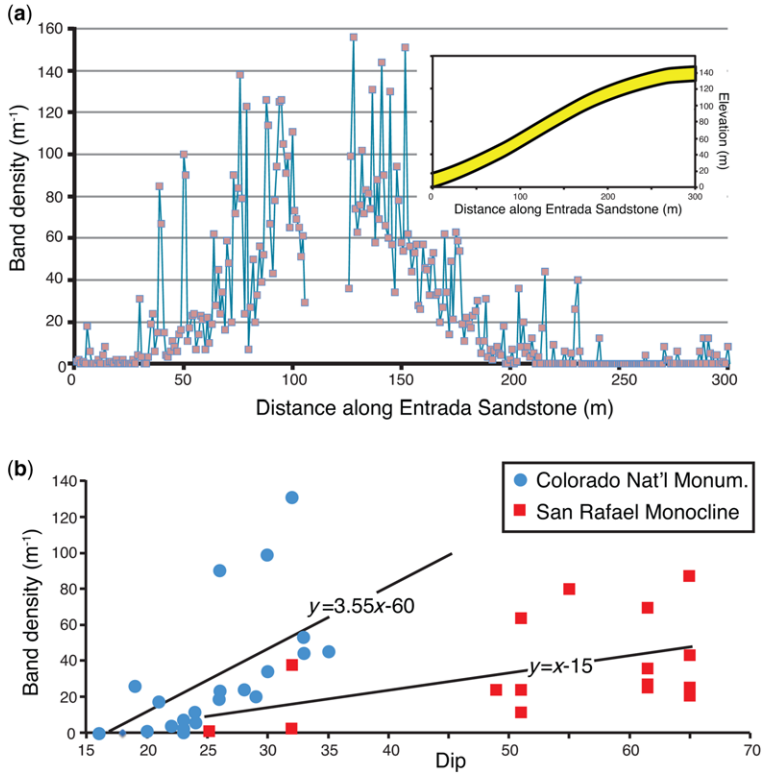

Fig. 17. Data from a monoclinal fold near Colorado National Monument, USA. Measurements are made in the Entrada Sandstone, whose bed geometry is shown in the inset constructed cross-section together with its slope values. The main graph in (**a**) shows band density along the layer, with a clear increase to the maximum around 150 m where the bedding is steepest. (**b**) There is a clear relation between bed dip and band density, but the exact relation depends to a large extent on lithological properties. Data from the San Rafael Reef (squares) therefore show a lower slope and a higher dip before deformation bands initiate. Data from Rønnevik (2013) and Zuluaga *et al.* (2012).

cases, pressure solution is important as an additional compaction mechanism. Furthermore, porosity- and permeability-reduction by post-tectonic precipitation of minerals can be promoted by the many fresh surfaces created during cataclasis.

Some important factors influencing cataclasis have already been discussed, and are listed in Figure 6. In general, the intensity of cataclasis increases with burial depth due to the increase in stress across grain contacts from the overburden and lithification, but the many other factors influencing this deformation mechanism complicate the picture. A compilation of permeability data is presented in Figure 19. The data show a wide range of values, from practically no permeability change through up to six orders of magnitude reduction in permeability. Ballas *et al.* (2015) presented a statistical treatment of the data shown in Figure 19, revealing significant differences between different kinds of bands and band clusters: PCB and SECB have the least cataclasis and therefore the least permeability-reducing effect, while slipped deformation bands and bands occurring in fault cores have the largest effect.

The practical effect of permeability reductions across deformation bands and band clusters also depends on their cumulative thickness. Even though SECB may involve a smaller reduction in porosity and permeability, the fact that they tend to be thicker adds to their ability to reduce the effective flow, for instance, between an injecting and a producing well (Fossen & Bale 2007; Saillet & Wibberley 2013). However, CSB are typically more laterally and vertically extensive than SECB, and may therefore have a more pervasive impact on reservoir permeability.

Even if deformation bands are unable to completely compartmentalize or seal reservoirs, the three-dimensional permeability anisotropy that they introduce, which depends on both petrophysical properties and band orientation, may be of some importance. In the simple case of conjugate sets (Fig. 1d) the preferred flow direction is parallel

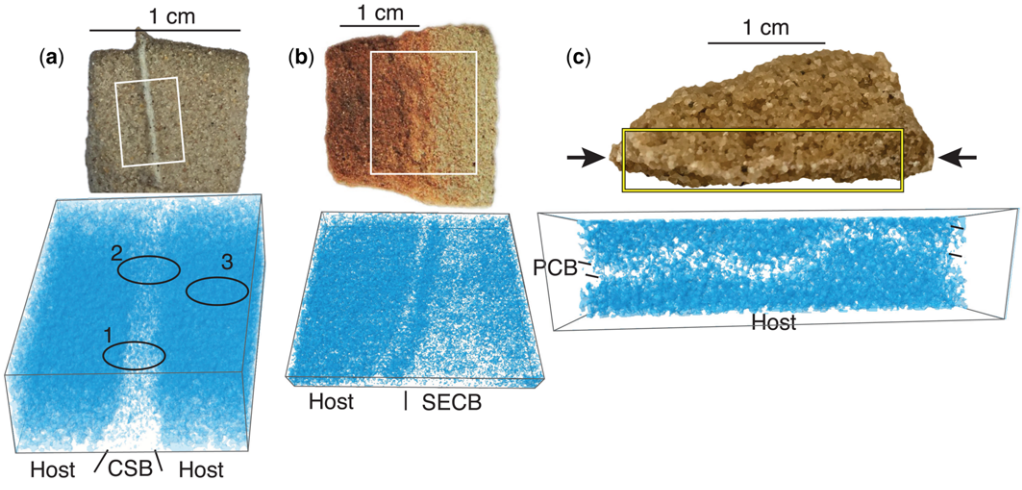

Fig. 18. Samples of the three main types of deformation bands involving cataclastic deformation and compaction, and 3D microCT models of a volume of each sample (indicated by rectangle). Each model shows pores (blue) and mineral phases (white), and therefore visualizes the porosity of the bands. (**a**) Single CSB from Entrada Sst near Goblin Valley, San Rafael Desert, Utah (see text for discussion of regions 1–3). (**b**) SECB from the Buffington Window (Muddy Mountains) near Valley of Fire State Park, Nevada. (**c**) PCB (sinusoidal) from highly porous sandstone layer in Buckskin Gulch, southern Utah. Note variations in amount of pores (porosity) along and within all the bands.

to the line of intersection between the sets, which is generally parallel to the strike of the nearest associated fault (Fossen & Bale 2007). Where the bands deviate from the conjugate (bimodal) to a more complex polymodal pattern, the anisotropy is reduced and the effect of the bands is to reduce the general flow rate.

In terms of distribution, bands in the extensional regime are typically clustered around faults. For example, Hesthammer & Fossen (2001) found that *c.* 75% of all deformation bands in the Gullfaks Oilfield in the North Sea were located in the damage zones of faults. Because most deformation bands in the extensional regime are components of fault structures and many wells are intentionally placed away from seismically resolvable faults and their damage zones, they do not usually affect production significantly. The main exception to this general rule reflects the fact that deformation bands also extend beyond the tips of faults as fault tip damage zones; this may help compartmentalize some reservoirs, or influence the flow pattern around fault tips as simulated by Rotevatn & Fossen (2011). This is in contrast to fault-damage zones in fractured reservoirs, where fractures can provide hydrocarbon storage and increased recovery for wells that intersect them (e.g. Hennings *et al.* 2012).

In the contractional regime, bands are much more evenly distributed throughout the reservoir and, to a much lesser extent, associated with faults (Soliva *et al.* 2016). They may therefore affect fluid flow in a different way from the clustered bands in the extensional regime, but not necessarily in a negative way. In this context it is interesting to note that SECB and PCB formed during contraction tend to be strongly dependent on lithology, in the sense that they only form in highly porous and coarse-grained parts of sandstone reservoirs and slow down the flow rate through these parts of the reservoir (Fossen *et al.* 2011). These porosity-sensitive bands would therefore homogenize the reservoir macro-permeability and thereby potentially improve the sweep.

Concluding remarks

Deformation bands are common constituents in deformed porous sandstone reservoirs and represent porosity- and permeability-reducing tabular elements where compaction is involved. It is useful to separate compactional bands into three distinct types which differ with respect to thickness, properties, geometry and distribution, and form under different stress states and lithological conditions. Data presented here suggest that CSB (compactional shear bands) form where porosity at the time of deformation was $\geq$15%, SECB (shear-enhanced compaction bands) require higher porosities ($>$20–25%) and PCB (pure compaction bands) require porosities close to 30%, although the exact

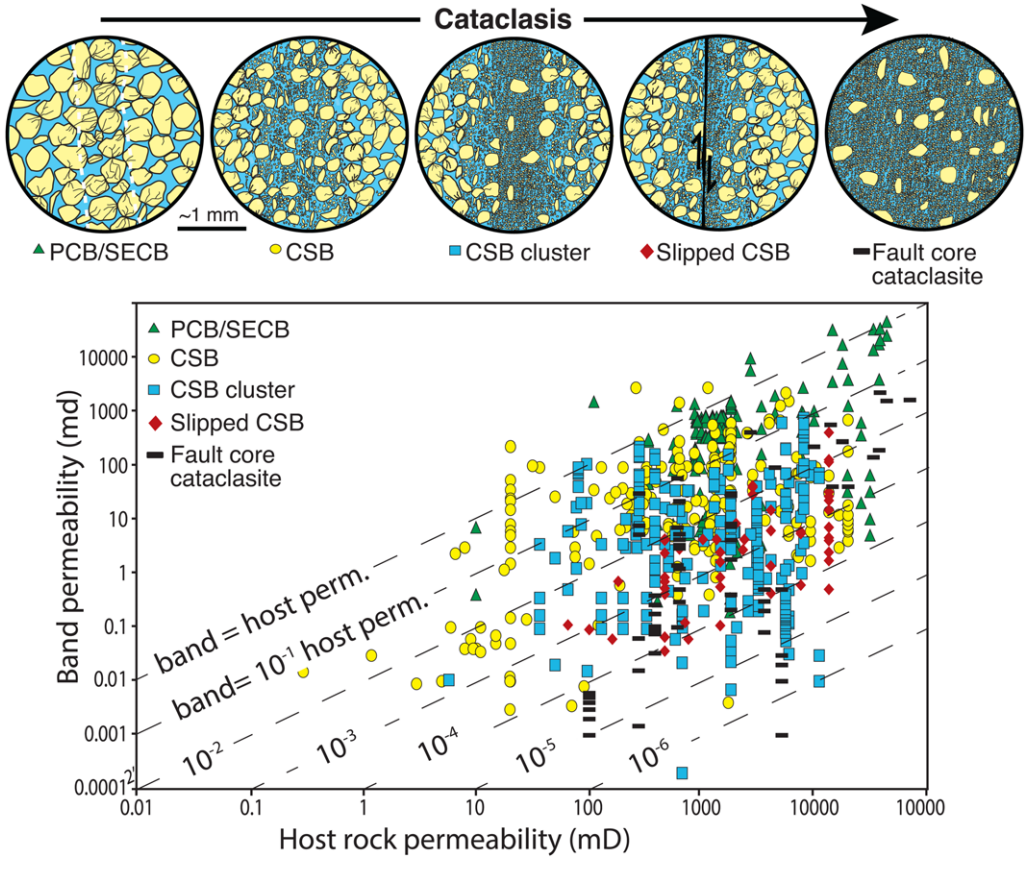

Fig. 19. Graph showing the relation between host-rock permeability and band permeability. The data show a large variation in permeability reduction, from 0 to 6 orders of magnitude depending on the type of data. The relative amount of cataclasis and therefore fluid-flow-reducing properties of each class of structure is illustrated above the graph. See Ballas *et al.* (2015) for more information.

cut-offs may vary according to other lithological parameters. SECB and PCB form under low differential stress most easily obtained in the contractional regime, while CSB can form in any tectonic setting. SECB show less cataclasis than CSB, and therefore reduce permeability to a lesser extent.

All categories of deformation bands tend to show systematic orientations that can be related to the local principal strain or stress axes. The simplest pattern is conjugate sets with acute angles that are higher for SECB (typically 80–90°) than for CSB (typically 40–50° in the extensional regime, around 60° in the contractional regime). Where the orientations of the principal stresses are known or can be inferred, deformation band orientations can to some extent be predicted and implemented into reservoir models. However, bands developing prior to fault formation in an area may have different orientations from those forming at a later stage, because of the stress-perturbations around and between faults. Maerten *et al.* (2006) modelled such stress perturbations to predict the orientations of subseismic faults in a part of the North Sea rift, and a similar approach can be used to predict the orientation of conjugate sets of CSB and therefore their influence on fluid flow during production.

In general, deformation bands introduce a permeability anisotropy to the reservoir or parts of the reservoir, whereas they do not tend to have sealing properties. When considering their role in hydrocarbon reservoirs, it is important to evaluate each reservoir separately in terms of the many parameters and conditions that influence how frequent deformation bands are, where they occur relative to larger structures, the type(s) of band, their permeability-reducing properties, and their lateral and vertical continuity. The most important variable is probably the amount of cataclasis involved,

because it is directly related to the reduction in porosity and permeability.

This work was supported by FAPESP Project 2015/23572/5 for the first author. We are grateful to reviewers Sarah Tindall and Adrian Neal for very helpful reviews, and to Mike Ashton for editorial handling.

References

Antonellini, M. & Aydin, A. 1995. Effect of faulting on fluid flow in porous sandstones: geometry and spatial distribution. *American Association of Petroleum Geologists Bulletin*, **79**, 642–671.

Antonellini, M. & Pollard, D.D. 1995. Distinct element modeling of deformation bands in sandstone. *Journal of Structural Geology*, **17**, 1165–1182.

Antonellini, M.A., Aydin, A. & Pollard, D.D. 1994. Microstructure of deformation bands in porous sandstones at Arches National Park, Utah. *Journal of Structural Geology*, **16**, 941–959.

Antonellini, M.A., Aydin, A. & Orr, L. 1999. Outcrop aided characterization of a faulted hydrocarbon reservoir: Arroyo Grande oil field, California, USA. *In*: Haneberg, W.C., Mozley, P.S., Moore, C.J. & Goodwin, L.B. (eds) *Faults and Subsurface Fluid Flow*. American Geophysical Union, Washington, Geophysical Monograph, **113**, 7–26.

Aydin, A. 1978. Small faults formed as deformation bands in sandstone. *Pure and Applied Geophysics*, **116**, 913–930.

Aydin, A. & Johnson, A.M. 1978. Development of faults as zones of deformation bands and as slip surfaces in sandstones. *Pure and Applied Geophysics*, **116**, 931–942.

Aydin, A. & Johnson, A.M. 1983. Analysis of faulting in porous sandstones. *Journal of Structural Geology*, **5**, 19–31.

Aydin, A. & Reches, Z. 1982. The number and orientation of fault sets in the field and in experiments. *Geology*, **10**, 107–112.

Aydin, A., Borja, R.I. & Eichhubl, P. 2006. Geological and mathematical framework for failure modes in granular rock. *Journal of Structural Geology*, **28**, 83–98.

Ballas, G., Soliva, R., Sizun, J.-P., Benedicto, A., Cavailhes, T. & Raynaud, S. 2012. The importance of the degree of cataclasis in shear bands for fluid flow in porous sandstone, Provence, France. *American Association of Petroleum Geologists Bulletin*, **96**, 2167–2186.

Ballas, G., Soliva, R., Sizun, J.-P., Fossen, H., Benedicto, A. & Skurtveit, E. 2013. Shear-enhanced compaction bands formed at shallow burial conditions; implications for fluid flow (Provence, France). *Journal of Structural Geology*, **47**, 3–15.

Ballas, G., Soliva, R., Benedicto, A. & Sizun, J.-P. 2014. Control of tectonic setting and large-scale faults on the basin-scale distribution of deformation bands in porous sandstone (Provence, France). *Marine and Petroleum Geology*, **55**, 142–159.

Ballas, G., Fossen, H. & Soliva, R. 2015. Factors controlling permeability of cataclastic deformation bands and faults in porous sandstone reservoirs. *Journal of Structural Geology*, **76**, 1–21.

Brandenburg, J.P., Alpak, F.O., Solum, J.G. & Naruk, S.J. 2012. A kinematic trishear model to predict deformation bands in a fault-propagation fold, East Kaibab monocline, Utah. *American Association of Petroleum Geologists Bulletin*, **96**, 109–132.

Chemenda, A.I., Ballas, G. & Soliva, R. 2014. Impact of a multilayer structure on initiation and evolution of strain localization in porous rocks: field observations and numerical modeling. *Tectonophysics*, **631**, 29–36.

Cheung, C.S.N., Baud, P. & Wong, T. 2012. Effect of grain size distribution on the development of compaction localization in porous sandstone. *Geophysical Research Letters*, **39**, L21302, https://doi.org/10.1029/2012GL053739

Cilona, A., Baud, P., Tondi, E., Agosta, F., Vinciguerra, S., Rustichelli, A. & Spiers, C.J. 2012. Deformation bands in porous carbonate grainstones: field and laboratory observations. *Journal of Structural Geology*, **45**, 137–157.

Cobbold, P.R. 1977. Description and origin of banded deformation structures. II. Rheology and the growth of banded perturbations. *Canadian Journal of Earth Science*, **14**, 2510–2523.

Davis, G.H. 1999. Structural geology of the Colorado Plateau Region of southern *Utah*. *Geological Society of America, Special Papers*, **342**, 1–157.

Davis, G.H., Reynholds, S.J. & Kluth, C.F. 2012. *Structural Geology of Rocks and Regions*. 3rd edn. Wiley, New York.

Du Bernard, X., Eichhubl, P. & Aydin, A. 2002. Dilation bands: a new form of localized failure in granular media. *Geophysical Research Letters*, **29**, 2176–2179.

Eichhubl, P., Hooker, J. & Laubach, S.E. 2010. Pure and shear-enhanced compaction bands in Aztec Sandstone. *Journal of Structural Geology*, **32**, 1873–1886.

Fisher, Q.J. & Knipe, R.J. 2001. The permeability of faults within siliciclastic petroleum reservoirs of the North Sea and Norwegian Continental Shelf. *Marine and Petroleum Geology*, **18**, 1063–1081.

Fossen, H. 2010. Deformation bands formed during soft-sediment deformation: observations from SE Utah. *Marine and Petroleum Geology*, **27**, 215–222.

Fossen, H. 2016. *Structural Geology*. 2nd edn. Cambridge University Press, Cambridge.

Fossen, H. & Bale, A. 2007. Deformation bands and their influence on fluid flow. *American Association of Petroleum Geologists Bulletin*, **91**, 1685–1700.

Fossen, H. & Gabrielsen, R.H. 2005. *Strukturgeologi*. Fagbokforlaget, Bergen.

Fossen, H. & Hesthammer, J. 1997. Geometric analysis and scaling relations of deformation bands in porous sandstone. *Journal of Structural Geology*, **19**, 1479–1493.

Fossen, H. & Rotevatn, A. 2012. Characterization of deformation bands associated with normal and reverse stress states in the Navajo Sandstone, Utah: discussion. *American Association of Petroleum Geologists Bulletin*, **96**, 869–876.

Fossen, H., Johansen, S.E., Hesthammer, J. & Rotevatn, A. 2005. Fault interaction in porous sandstone and implications for reservoir management; examples

from southern Utah. *American Association of Petroleum Geologists Bulletin*, **89**, 1593–1606.

Fossen, H., Schultz, R.A., Shipton, Z.K. & Mair, K. 2007. Deformation bands in sandstone - a review. *Journal of the Geological Society, London*, **164**, 755–769.

Fossen, H., Schultz, R.A. & Torabi, A. 2011. Conditions and implications for compaction band formation in the Navajo Sandstone, Utah. *Journal of Structural Geology*, **33**, 1477–1490.

Fossen, H., Zuluaga, L.F., Ballas, G., Soliva, R. & Rotevatn, A. 2015. Contractional deformation of porous sandstone: insights from the Aztec Sandstone, SE Nevada, USA. *Journal of Structural Geology*, **74**, 172–184.

Grueschow, E. & Rudnicki, J.W. 2005. Elliptic yield cap constitutive modeling for high porosity sandstone. *International Journal of Solids and Structures*, **42**, 4574–4587, https://doi.org/10.1016/j.ijsolstr.2005.02.001

Hancock, P.L. 1985. Brittle microtectonics: principles and practice. *Journal of Structural Geology*, **7**, 437–457.

Healy, D., Blenkinsop, T.G., Timms, N.E., Meredith, P.G., Mitchell, T.M. & Cooke, M.L. 2015. Polymodal faulting: time for a new angle on shear failure. *Journal of Structural Geology*, **80**, 57–71.

Hennings, P., Allwardt, P., *et al.* 2012. Relationship between fractures, fault zones, stress and reservoir productivity in the Suban gas field, Sumatra, Indonesia. *American Association of Petroleum Geologists Bulletin*, **96**, 753–772.

Hesthammer, J. & Fossen, H. 2001. Structural core analysis from the Gullfaks area, northern North Sea. *Marine and Petroleum Geology*, **18**, 411–439.

Johansen, S.E. & Fossen, H. 2008. Internal geometry of fault damage zones in siliclastic rocks. *In*: Kurz, W., Wibberley, C.A.J., Imber, J., Collettini, C. & Holdsworth, R.E. (eds) *The Internal Structure of Fault Zones: Implications for Mechanical and Fluid Flow Properties*. Geological Society, London, Special Publications, **299**, 35–56.

Klimczak, C. & Schultz, R.A. 2013. Localized compaction in dilating materials. *International Journal of Rock Mechanics and Mining Sciences*, **64**, 139–147.

Klimczak, C., Soliva, R., Schultz, R.A. & Chéry, J. 2011. Sequential growth of deformation bands in a multilayer sequence. *Journal of Geophysical Research*, **116**, https://doi.org/10.1029/2011jb008365

Knipe, R.J., Fisher, Q.J. *et al.* 1997. Fault seal analysis: successful methodologies, application and future directions. *In*: MøllerPedersen, P. & Koestler, A.G. (eds) *Hydrocarbon Seals: Importance for Exploration and Production*. Norwegian Petroleum Society, Bergen, Special Publications, **7**, 15–40.

Lewis, H. & Couples, G.D. 1993. Production evidence for geological heterogeneities in the Anschutz Ranch East Field, western USA. *In*: North, C.P. & Prosser, D.J. (eds) *Characterization of Fluvial and Aeolian Reservoirs*. Geological Society, London, Special Publications, **73**, 321–338.

Liu, C., Pollard, D.D., Deng, S. & Aydin, A. 2016. Mechanism of formation of wiggly compaction bands in porous sandstone: 1. Observations and conceptual model. *Journal of Geophysical Research Solid Earth*, **120**, 8138–8152, https://doi.org/10.1002/2015JB012372

Maerten, L., Gillespie, P. & Daniel, J.-M. 2006. T-hree-dimensional geomechanical modeling for constraint of subseismic fault simulation. *American Association of Petroleum Geologists Bulletin*, **90**, 1337–1358.

Mollema, P.N. & Antonellini, M.A. 1996. Compaction bands: a structural analog for anti-mode I cracks in aeolian sandstone. *Tectonophysics*, **267**, 209–228.

Nicol, A., Childs, C., Walsh, J.J. & Schafer, K.W. 2013. A geometric model for the formation of deformation band clusters. *Journal of Structural Geology*, **55**, 21–33.

Ngwenya, B.T., Elphick, S.C., Main, I.G. & Shimmield, G.B. 2000. Experimental constraints on the diagenetic self-sealing capasity of faults in high porosity rocks. *Earth and Planetary Science Letters*, **183**, 187–199.

Passchier, C.W. & Trouw, R.A.J. 2005. *Microtectonics*. 2nd edn. Springer, Berlin.

Philit, S., Soliva, R., Labaume, P., Gout, C. & Wibberley, C. 2015. Relations between shallow cataclastic faulting and cementation in porous sandstones: first insight from a groundwater environmental context. *Journal of Structural Geology*, **81**, 89–105.

Rawling, G.C. & Goodwin, L.B. 2003. Cataclasis and particulate flow in faulted, poorly lithified sediments. *Journal of Structural Geology*, **25**, 317–331.

Rieke, H.H. & Chilingarian, G.V. 1974. *Compaction of Argillaceous Sediments*. Amsterdam, Elsevier, *Developments in Sedimentology*, **16**, 424 pp.

Rodrigues, M.C.N.d.L., Trzaskos, B. & Lopes, A.P. 2015. Influence of deformation bands on sandstone porosity: a case study using three-dimensional microtomography. *Journal of Structural Geology*, **72**, 96–110.

Rønnevik, C. 2013. *Low-temperature thermochronology apatite fission-track (AFT) study and structural relations associated with the Uncompahgre Plateau and Paradox Basin area, Utah and Colorado, USA*. Masters thesis, Department of Earth Science, University of Bergen.

Rotevatn, A. & Fossen, H. 2011. Simulating the effect of subseismic fault tails and process zones in a siliciclastic reservoir analogue: implications for aquifer support and trap definition. *Marine and Petroleum Geology*, **28**, 1648–1662.

Rotevatn, A., Tveranger, J., Howell, J.A. & Fossen, H. 2009. Dynamic investigation of the effect of a relay ramp on simulated fluid flow: geocellular modelling of the Delicate Arch Ramp, Utah. *Petroleum Geoscience*, **15**, 45–58.

Rotevatn, A., Torabi, A., Fossen, H. & Braathen, A. 2008. Slipped deformation bands: a new type of cataclastic deformation bands in Western Sinai, Suez rift, Egypt. *Journal of Structural Geology*, **30**, 1317–1331.

Rotevatn, A., Sandve, T.H., Keilegavlen, E., Kolyukhin, D. & Fossen, H. 2013. Deformation bands and their impact on fluid flow in sandstone reservoirs: the role of natural thickness variations. *Geofluids*, **13**, 359–371, https://doi.org/10.1111

Rudnicki, J.W. & Rice, J.R. 1975. Conditions for the localization of deformation in pressure-sensitive

dilatant materials. *Journal of the Mechanics and Physics of Solids*, **23**, 371–394.

Saillet, E. & Wibberley, C.A.J. 2013. Permeability and flow impact of faults and deformation bands in high-porosity sand reservoirs: Southeast Basin, France, analog. *American Association of Petroleum Geologists Bulletin*, **97**, 437–464.

Schueller, S., Braathen, A., Fossen, H. & Tveranger, J. 2013. Spatial distribution of deformation bands in damage zones of extensional faults in porous sandstones: statistical analysis of field data. *Journal of Structural Geology*, **52**, 148–162.

Schultz, R.A. 2009. Scaling and paleodepth of compaction bands, Nevada and Utah. *Journal of Geophysical Research*, **114**, B03407, https://doi.org/10.1029/2008JB005876

Schultz, R.A. & Balasko, C.M. 2003. Growth of deformation bands into echelon and ladder geometries. *Geophysical Research Letters*, **30**, https://doi.org/10.1029/2003GL018449.

Schultz, R.A. & Siddharthan, R. 2005. A general framework for the occurrence and faulting of deformation bands in porous granular rocks. *Tectonophysics*, **411**, 1–18.

Schultz, R.A., Soliva, R., Fossen, H., Okubo, C.H. & Reeves, D.M. 2008. Dependence of displacement–length scaling relations for fractures and deformation bands on the volumetric changes across them. *Journal of Structural Geology*, **30**, 1405–1411.

Schultz, R.A., Okubo, C.H. & Fossen, H. 2010. Porosity and grain size controls on compaction band formation in Jurassic Navajo Sandstone. *Geophysical Research Letters*, **37**, L22306, https://doi.org/10.1029/2010GL044909

Shipton, Z.K. & Cowie, P.A. 2001. Analysis of three-dimensional damage zone development over μm to km scale range in the high-porosity Navajo sandstone, Utah. *Journal of Structural Geology*, **23**, 1825–1844.

Shipton, Z.K. & Cowie, P.A. 2003. A conceptual model for the origin of fault damage zone structures in high-porosity sandstone. *Journal of Structural Geology*, **25**, 333–345.

Soliva, R., Schultz, R.A., Ballas, G., Taboada, A., Wibberley, C., Saillet, E. & Benedicto, A. 2013. A model of strain localization in porous sandstone as a function of tectonic setting, burial and material properties; new insight from Provence (southern France). *Journal of Structural Geology*, **49**, 50–63.

Soliva, R., Ballas, G., Fossen, H. & Philit, S. 2016. Tectonic regime controls clustering of deformation bands in porous sandstone. *Geology*, **44**, 423–426.

Sternlof, K., Rudnicki, J.W. & Pollard, D.D. 2005. Anticrack inclusion model for compaction bands in sandstone. *Journal of Geophysical Research*, **110**, B11403, https://doi.org/10.1029/2005JB003764

Sternlof, K., Karimi-Fard, M. & Durlofsky, L.J. 2006. Flow and transport effects of compaction bands in sandstone at scales relevant to aquifer and reservoir management. *Water Resources Research*, **42**, 16.

Tikoff, B. & Wojtal, S.F. 1999. Displacement control of geologic structures. *Journal of Structural Geology*, **21**, 959–967.

Tindall, S.E. 2006. Jointed deformation bands may not compartmentalize reservoirs. *American Association of Petroleum Geologists Bulletin*, **90**, 177–192.

Torabi, A. & Fossen, H. 2009. Spatial variation of microstructure and petrophysical properties along deformation bands in reservoir sandstones. *American Association of Petroleum Geologists Bulletin*, **93**, 919–938.

Torabi, A., Fossen, H. & Braathen, A. 2013. Insight into petrophysical properties of deformed sandstone reservoirs. *American Association of Petroleum Geologists Bulletin*, **97**, 619–637.

Underhill, J.R. & Woodcock, N.H. 1987. Faulting mechanisms in high-porosity sandstones: New Red Sandstone, Arran, Scotland. *In*: Jones, M.E. & Preston, R.M.F. (eds) *Deformation of Sediments and Sedimentary Rocks*. Geological Society, London, Special Publications, **29**, 91–105.

Wibberley, C.A.J., Petit, J.-P. & Rives, T. 2007. The mechanics of fault distribution & localization in high-porosity sands, Provence, France. *In*: Lewis, H. & Couples, G.D. (eds) *The Relationship between Damage & Localization*. Geological Society, London, Special Publications, **289**, 19–46.

Wong, T.-F., David, C. & Zhu, Q. 1997. The transition from brittle faulting to cataclastic flow in porous sandstones: mechanical deformation. *Journal of Geophysical Research*, **102**, 3009–3025.

Zhang, J., Wong, T.-F. & Davis, D.M. 1990. Micromechanics of pressure-induced grain crushing in porous rocks. *Journal of Geophysical Research*, **95**, 341–352.

Zuluaga, L.F., Fossen, H. & Rotevatn, A. 2012. Structural reservoir heterogeneity induced by forced folding in sandstone reservoirs: the San Rafael Reef Monocline, Utah, USA. *The Geological Society (Petroleum Group/Tectonic Studies Group Conference)*, London, 28–30 November 2012.

Zuluaga, L.F., Fossen, H. & Rotevatn, A. 2014. Progressive evolution of deformation band populations during Laramide fault-propagation folding: Navajo Sandstone, San Rafael monocline, Utah, U.S.A. *Journal of Structural Geology*, **68**, 66–81.